Sliced Score Matching: A Scalable Approach to Density and Score Estimation

Yang Song[*]
Stanford University

Sahaj Garg[*]
Stanford University

Jiaxin Shi
Tsinghua University

Stefano Ermon
Stanford University

Abstract

Score matching is a popular method for estimating unnormalized statistical models. However, it has been so far limited to simple models or low-dimensional data, due to the difficulty of computing the trace of Hessians for log-density functions. We show this difficulty can be mitigated by *sliced score matching*, a new objective that matches random projections of the original scores. Our objective only involves Hessian-vector products, which can be easily implemented using reverse-mode auto-differentiation. This enables scalable score matching for complex models and higher dimensional data. Theoretically, we prove the consistency and asymptotic normality of sliced score matching. Moreover, we demonstrate that sliced score matching can be used to learn deep score estimators for implicit distributions. In our experiments, we show that sliced score matching greatly outperforms competitors on learning deep energy-based models, and can produce accurate score estimates for applications such as variational inference with implicit distributions and training Wasserstein Auto-Encoders.

1 INTRODUCTION

Score matching (Hyvärinen, 2005) is a statistical estimation method particularly suitable for learning unnormalized models. Unlike maximum likelihood estimation (MLE), the objective of score matching only depends on the derivative of the log-density function (a.k.a., *score*), which is independent of the normalizing term. However,

score matching has been so far limited to small density models and low-dimensional data, because its objective involves the trace of the Hessian for the log-density function, which is expensive to compute for general densities (Martens et al., 2012), and especially those parameterized by neural networks, such as deep energy-based models (LeCun et al., 2006; Wenliang et al., 2018).

There are several attempts to alleviate this difficulty: Kingma & LeCun (2010) proposes approximate backpropagation for computing the trace of the Hessian; Martens et al. (2012) develops curvature propagation, a fast stochastic estimator for the trace in score matching; and Vincent (2011) transforms score matching to a denoising problem which avoids second-order derivatives. These methods have achieved some success, but may suffer from one or many of the following problems: inconsistent parameter estimation, large estimation variance, and cumbersome implementation.

To avoid these problems, we propose *sliced score matching*, a variant of score matching that can scale up to large unnormalized models and high dimensional data. The key intuition is that instead of directly matching the high-dimensional scores, we match their projections along random directions. Our theoretical results show that under some regularity conditions, sliced score matching is a well-defined statistical estimation criterion that yields consistent and asymptotically normal parameter estimates. Moreover, compared to the methods of Kingma & LeCun (2010) and Martens et al. (2012), whose implementations require customized backpropagation for deep networks, the objective of sliced score matching only involves Hessian-vector products, thus can be easily implemented in automatic differentiation frameworks such as TensorFlow (Abadi et al., 2016) and PyTorch (Adam et al., 2017).

Since score matching is based on the distance between model and data scores, it can be naturally used as an objective for estimating data score functions (Sasaki et al.,

---

[*]Joint first authors. Correspondence to Yang Song <yangsong@cs.stanford.edu> and Stefano Ermon <ermon@cs.stanford.edu>.

2014; Strathmann et al., 2015). We show that given a set of samples, sliced score matching can be used to train a deep neural network as a score estimator. This observation opens up a new direction of applications for sliced score matching. For example, we show that sliced score estimation can be used to provide accurate score estimates for many tasks, such as variational inference with implicit distributions (Huszár, 2017) and learning Wasserstein Auto-Encoders (WAE) (Tolstikhin et al., 2018).

Finally, we evaluate the performance of sliced score matching on both density and score estimation tasks. For density estimation, experiments on deep kernel exponential families (Wenliang et al., 2018) and NICE flow models (Dinh et al., 2015) show that our method is either more scalable or more accurate than existing score matching variants. When applied to score estimation, our method improves the performance of variational auto-encoders (VAE) with implicit encoders, and can train WAEs without a discriminator or MMD loss by directly optimizing the KL divergence between aggregated posteriors and the prior. In both situations we outperformed kernel-based score estimators (Li & Turner, 2018; Shi et al., 2018) by achieving better test likelihoods and better qualities of random image generation.

2 BACKGROUND

Given i.i.d. samples from a data distribution $p_d(\mathbf{x})$, our task is to learn an unnormalized density, $\tilde{p}_m(\mathbf{x}; \boldsymbol{\theta})$, where $\boldsymbol{\theta}$ is from some parameter space Θ. The model's normalizing constant (a.k.a., partition function) is denoted as $Z_{\boldsymbol{\theta}}$, which is assumed to be intractable. A deep energy-based model is an unnormalized model that uses a deep feedforward neural network to parameterize $\log \tilde{p}_m(\mathbf{x}; \boldsymbol{\theta})$. Let $p_m(\mathbf{x}; \boldsymbol{\theta})$ be the normalized density determined by our model, we have

$$p_m(\mathbf{x}; \boldsymbol{\theta}) = \frac{\tilde{p}_m(\mathbf{x}; \boldsymbol{\theta})}{Z_{\boldsymbol{\theta}}}, \quad Z_{\boldsymbol{\theta}} = \int \tilde{p}_m(\mathbf{x}; \boldsymbol{\theta}) \mathrm{d}\mathbf{x}.$$

For convenience, we denote the (Stein) score function as $\mathbf{s}(\mathbf{x}) \triangleq \nabla_{\mathbf{x}} \log p(\mathbf{x}; \boldsymbol{\theta})$, which is the gradient of the log-density function w.r.t. the data point. Note that since $\log p_m(\mathbf{x}; \boldsymbol{\theta}) = \log \tilde{p}_m(\mathbf{x}; \boldsymbol{\theta}) - \log Z_{\boldsymbol{\theta}}$, we immediately conclude that the score function of our model $\mathbf{s}_m(\mathbf{x}; \boldsymbol{\theta}) = \nabla_{\mathbf{x}} \log p_m(\mathbf{x}; \boldsymbol{\theta}) = \nabla_{\mathbf{x}} \log \tilde{p}_m(\mathbf{x}; \boldsymbol{\theta})$ does not depend on the intractable partition function $Z_{\boldsymbol{\theta}}$.

2.1 SCORE MATCHING

Learning unnormalized models with maximum likelihood estimation (MLE) is difficult because of the intractability of the partition function $Z_{\boldsymbol{\theta}}$. To avoid the partition function, score matching (Hyvärinen, 2005) minimizes the Fisher divergence between p_d and $p_m(\cdot, \boldsymbol{\theta})$, which is defined as

$$L(\boldsymbol{\theta}) \triangleq \frac{1}{2} \mathbb{E}_{p_d}[\|\mathbf{s}_m(\mathbf{x}; \boldsymbol{\theta}) - \mathbf{s}_d(\mathbf{x})\|_2^2]. \tag{1}$$

Since $\mathbf{s}_m(\mathbf{x}; \boldsymbol{\theta})$ is independent of $Z_{\boldsymbol{\theta}}$, the Fisher divergence avoids the intractable partition function. However, Eq. (1) is still not readily usable for learning unnormalized models, as we usually do not have access to the score function of the data $\mathbf{s}_d$.

By applying integration by parts, Hyvärinen (2005) shows that $L(\boldsymbol{\theta})$ can be written as (*cf*., Theorem 1 in Hyvärinen (2005)):

$$L(\boldsymbol{\theta}) = \mathbb{E}_{p_d}\left[\mathrm{tr}(\nabla_{\mathbf{x}} \mathbf{s}_m(\mathbf{x}; \boldsymbol{\theta})) + \frac{1}{2} \|\mathbf{s}_m(\mathbf{x}; \boldsymbol{\theta})\|_2^2 \right] + \mathrm{C} \tag{2}$$

where C is a constant that does not depend on θ, $\mathrm{tr}(\cdot)$ denotes the trace of a matrix, and

$$\nabla_{\mathbf{x}} \mathbf{s}_m(\mathbf{x}; \boldsymbol{\theta}) = \nabla_{\mathbf{x}}^2 \log \tilde{p}_m(\mathbf{x}; \boldsymbol{\theta}) \tag{3}$$

is the Hessian of the log-density function. The constant can be ignored and the following unbiased estimator of the remaining terms is used to train our unnormalized model:

$$\hat{J}(\boldsymbol{\theta}; \mathbf{x}_1^N) \triangleq \frac{1}{N} \sum_{i=1}^{N} \left[\mathrm{tr}(\nabla_{\mathbf{x}} \mathbf{s}_m(\mathbf{x}_i; \boldsymbol{\theta})) + \frac{1}{2} \|\mathbf{s}_m(\mathbf{x}_i; \boldsymbol{\theta})\|_2^2 \right],$$

where $\mathbf{x}_1^N$ is a shorthand used throughout the paper for a collection of N data points $\{\mathbf{x}_1, \mathbf{x}_2, \cdots, \mathbf{x}_N\}$ sampled i.i.d. from p_d.

Computational difficulty While the score matching objective $\hat{J}(\boldsymbol{\theta}; \mathbf{x}_1^N)$ avoids the computation of $Z_{\boldsymbol{\theta}}$ for unnormalized models, it introduces a new computational difficulty: computing the trace of the Hessian of a log-density function, $\nabla_{\mathbf{x}}^2 \log \tilde{p}_m$. Suppose that the input data $\mathbf{x}$ has dimension D. A naïve approach of computing the trace of the Hessian requires D times more backward passes than computing the gradient $\mathbf{s}_m = \nabla_{\mathbf{x}} \log \tilde{p}_m$ (see Alg. 2 in the appendix). For example, the trace could be computed by applying backpropagation D times to $\mathbf{s}_m$ to get each diagonal term of $\nabla_{\mathbf{x}}^2 \log \tilde{p}_m$ sequentially. In practice, D can be many thousands, which can render score matching too slow for practical purposes. Moreover, Martens et al. (2012) argues from a theoretical perspective that it is unlikely that there exists a computationally efficient algorithm (at the level of a constant number of forward and backward passes) for computing the diagonal of the Hessian defined by an arbitrary computation graph.

2.2 SCORE ESTIMATION FOR IMPLICIT DISTRIBUTIONS

Besides parameter estimation in unnormalized models, score matching can also be used to estimate scores of

implicit distributions, which are distributions that have a tractable sampling process but without a tractable density. Implicit distributions can arise in many situations such as the marginal distribution of a non-conjugate model (Sun et al., 2019), non-invertible transformation of random variables (Goodfellow et al., 2014), and models defined by complex simulation processes (Tran et al., 2017). In these cases learning and inference often become intractable due to the need of optimizing an objective that involves the intractable density.

In these cases, directly estimating the score function $\mathbf{s}_q(\mathbf{x}) = \nabla_{\mathbf{x}} \log q_{\boldsymbol{\theta}}(\mathbf{x})$ based on i.i.d. samples from an implicit density $q_{\boldsymbol{\theta}}(\mathbf{x})$ can be useful. For example, suppose our learning problem involves optimizing the entropy $H(q_{\boldsymbol{\theta}}(\mathbf{x}))$ of an implicit distribution. This situation is common when dealing with variational free energies (Kingma & Welling, 2014). Suppose $\mathbf{x} \sim q_{\boldsymbol{\theta}}$ can be reparameterized as $\mathbf{x} = g_{\boldsymbol{\theta}}(\boldsymbol{\epsilon})$, where $\boldsymbol{\epsilon}$ is a simple random variable independent of $\boldsymbol{\theta}$, such as a standard normal, and $g_{\boldsymbol{\theta}}$ is a deterministic mapping. We can write the gradient of the entropy with respect to $\boldsymbol{\theta}$ as

$$\begin{aligned}
\nabla_{\boldsymbol{\theta}} H(q_{\boldsymbol{\theta}}) &\triangleq -\nabla_{\boldsymbol{\theta}} \mathbb{E}_{q_{\boldsymbol{\theta}}(\mathbf{x})}[\log q_{\boldsymbol{\theta}}(\mathbf{x})] \\
&= -\nabla_{\boldsymbol{\theta}} \mathbb{E}_{p(\boldsymbol{\epsilon})}[\log q_{\boldsymbol{\theta}}(g_{\boldsymbol{\theta}}(\boldsymbol{\epsilon}))] \\
&= -\mathbb{E}_{p(\boldsymbol{\epsilon})}[\nabla_{\mathbf{x}} \log q_{\boldsymbol{\theta}}(\mathbf{x})|_{\mathbf{x}=g_{\boldsymbol{\theta}}(\boldsymbol{\epsilon})} \nabla_{\boldsymbol{\theta}} g_{\boldsymbol{\theta}}(\boldsymbol{\epsilon})],
\end{aligned}$$

where $\nabla_{\boldsymbol{\theta}} g_{\boldsymbol{\theta}}(\boldsymbol{\epsilon})$ is usually easy to compute. The score $\nabla_{\mathbf{x}} \log q_{\boldsymbol{\theta}}(\mathbf{x})$ is intractable but can be approximated by score estimation.

Score matching is an attractive solution for score estimation since (2) naturally serves as an objective if we replace $\mathbf{s}_d(\mathbf{x})$ with $\nabla_{\mathbf{x}} \log q_{\boldsymbol{\theta}}(\mathbf{x})$. There are also other kernel-based score estimators (Li & Turner, 2018; Shi et al., 2018) which we discuss in detail in section 5.2. Score estimation like this can be applied to training VAEs and WAEs, as we shall see in the experiments.

3 METHOD

In this section, we introduce *sliced score matching* (SSM), our scalable method designed for density and score estimation with deep energy-based models.

3.1 SLICED SCORE MATCHING

Our intuition is that one dimensional problems are usually much easier to solve than high dimensional ones. Inspired by the idea of Sliced Wasserstein distance (Rabin et al., 2012), we consider projecting $\mathbf{s}_d(\mathbf{x})$ and $\mathbf{s}_m(\mathbf{x}; \boldsymbol{\theta})$ onto some random direction $\mathbf{v}$ and propose to compare their average difference along that random direction. More specifically, we consider the following objective as a re-

placement of the Fisher divergence $L(\boldsymbol{\theta})$ in Eq. (1):

$$L(\boldsymbol{\theta}; p_{\mathbf{v}}) \triangleq \frac{1}{2} \mathbb{E}_{p_{\mathbf{v}}} \mathbb{E}_{p_d} \left[(\mathbf{v}^{\mathsf{T}} \mathbf{s}_m(\mathbf{x}; \boldsymbol{\theta}) - \mathbf{v}^{\mathsf{T}} \mathbf{s}_d(\mathbf{x}))^2 \right], \quad (4)$$

Here $\mathbf{v} \sim p_{\mathbf{v}}$ and $\mathbf{x} \sim p_d$ are independent, and we require $\mathbb{E}_{p_{\mathbf{v}}}[\mathbf{v}\mathbf{v}^{\mathsf{T}}] \succ 0$ and $\mathbb{E}_{p_{\mathbf{v}}}[\|\mathbf{v}\|_2^2] < \infty$. Many examples of $p_{\mathbf{v}}$ satisfy these requirements. For instance, $p_{\mathbf{v}}$ can be a multivariate standard normal ($\mathcal{N}(0, I_D)$), a multivariate Rademacher distribution (the uniform distribution over $\{\pm 1\}^D$), or a uniform distribution on the hypersphere $\mathbb{S}^{D-1}$ (recall that D refers to the dimension of $\mathbf{x}$).

To eliminate the dependence of $L(\boldsymbol{\theta}; p_{\mathbf{v}})$ on $\mathbf{s}_d(\mathbf{x})$, we use integration by parts as in score matching (*cf.*, the equivalence between Eq. (1) and (2)). Defining

$$\begin{aligned}
J(\boldsymbol{\theta}; p_{\mathbf{v}}) \triangleq \mathbb{E}_{p_{\mathbf{v}}} \mathbb{E}_{p_d} \big[&\mathbf{v}^{\mathsf{T}} \nabla_{\mathbf{x}} \mathbf{s}_m(\mathbf{x}; \boldsymbol{\theta}) \mathbf{v} \\
&+ \frac{1}{2} (\mathbf{v}^{\mathsf{T}} \mathbf{s}_m(\mathbf{x}; \boldsymbol{\theta}))^2 \big], \quad (5)
\end{aligned}$$

the equivalence is summarized in the following theorem.

Theorem 1. *Under some regularity conditions (Assumption 1-3), we have*

$$L(\boldsymbol{\theta}; p_{\mathbf{v}}) = J(\boldsymbol{\theta}; p_{\mathbf{v}}) + \mathrm{C}, \quad (6)$$

where C *is a constant w.r.t.* $\boldsymbol{\theta}$.

Other than our requirements on $p_{\mathbf{v}}$, the assumptions are exactly the same as in Theorem 1 of Hyvärinen (2005). We advise the interested readers to read Appendix B.2 for technical statements of the assumptions and a rigorous proof of the theorem.

In practice, given a dataset $\mathbf{x}_1^N$, we draw M projection vectors independently for each point $\mathbf{x}_i$. The collection of all such vectors are denoted as $\mathbf{v}_{11}^{NM}$. We then use the following unbiased estimator of $J(\boldsymbol{\theta}; p_{\mathbf{v}})$

$$\begin{aligned}
\hat{J}(\boldsymbol{\theta}; \mathbf{x}_1^N, \mathbf{v}_{11}^{NM}) \triangleq \frac{1}{N} \frac{1}{M} \sum_{i=1}^{N} \sum_{j=1}^{M} &\mathbf{v}_{ij}^{\mathsf{T}} \nabla_{\mathbf{x}} \mathbf{s}_m(\mathbf{x}_i; \boldsymbol{\theta}) \mathbf{v}_{ij} \\
&+ \frac{1}{2} \left(\mathbf{v}_{ij}^{\mathsf{T}} \mathbf{s}_m(\mathbf{x}_i; \boldsymbol{\theta}) \right)^2. \quad (7)
\end{aligned}$$

Note that when $p_{\mathbf{v}}$ is a multivariate standard normal or multivariate Rademacher distribution, we have $\mathbb{E}_{p_{\mathbf{v}}}[(\mathbf{v}^{\mathsf{T}} \mathbf{s}_m(\mathbf{x}; \boldsymbol{\theta}))^2] = \|\mathbf{s}_m(\mathbf{x}; \boldsymbol{\theta})\|_2^2$, in which case the second term of $J(\boldsymbol{\theta}; p_{\mathbf{v}})$ can be integrated analytically, and may lead to an estimator with reduced variance:

$$\begin{aligned}
\hat{J}_{\mathrm{vr}}(\boldsymbol{\theta}; \mathbf{x}_1^N, \mathbf{v}_{11}^{NM}) \triangleq \frac{1}{N} \frac{1}{M} \sum_{i=1}^{N} \sum_{j=1}^{M} &\mathbf{v}_{ij}^{\mathsf{T}} \nabla_{\mathbf{x}} \mathbf{s}_m(\mathbf{x}_i; \boldsymbol{\theta}) \mathbf{v}_{ij} \\
&+ \frac{1}{2} \|\mathbf{s}_m(\mathbf{x}_i; \boldsymbol{\theta})\|_2^2. \quad (8)
\end{aligned}$$

Empirically, we do find that $\hat{J}_{\mathrm{vr}}$ has better performance than $\hat{J}$. We refer to this version as sliced score matching with variance reduction (SSM-VR). In fact, we can leverage $\mathbb{E}_{p_\mathbf{v}}[(\mathbf{v}^\intercal\mathbf{s}_m(\mathbf{x};\boldsymbol{\theta}))^2] = \|\mathbf{s}_m(\mathbf{x};\boldsymbol{\theta})\|_2^2$ to create a control variate for guaranteed reduction of variance (Appendix D). $\hat{J}_{\mathrm{vr}}$ is also closely related to Hutchinson's trace estimator (Hutchinson, 1990), which we will analyze later in Section 4.3.

For sliced score matching, the second derivative term $\mathbf{v}^\intercal\nabla_\mathbf{x}\mathbf{s}_m(\mathbf{x};\boldsymbol{\theta})\mathbf{v}$ is much less computationally expensive than $\mathrm{tr}(\nabla_\mathbf{x}\mathbf{s}_m(\mathbf{x};\boldsymbol{\theta}))$. Using auto-differentiation systems that support higher order gradients, we can compute it using two gradient operations for a single $\mathbf{v}$, as shown in Alg. 1. Similarly, when there are M $\mathbf{v}$'s, the total number of gradient operations is $M + 1$. In contrast, assuming the dimension of $\mathbf{x}$ is D and $D \gg M$, we typically need $D + 1$ gradient operations to compute $\mathrm{tr}(\nabla_\mathbf{x}\mathbf{s}_m(\mathbf{x};\boldsymbol{\theta}))$ because each diagonal entry of $\nabla_\mathbf{x}\mathbf{s}_m(\mathbf{x};\boldsymbol{\theta})$ needs to be computed separately (see Alg. 2 in the appendix).

Algorithm 1 Sliced Score Matching

Input: $\tilde{p}_m(\cdot;\boldsymbol{\theta}), \mathbf{x}, \mathbf{v}$
1: $\mathbf{s}_m \leftarrow \mathrm{grad}(\log \tilde{p}_m(\mathbf{x};\boldsymbol{\theta}), \mathbf{x})$
2: $\mathbf{v}^\intercal\nabla_\mathbf{x}\mathbf{s}_m \leftarrow \mathrm{grad}(\mathbf{v}^\intercal\mathbf{s}_m, \mathbf{x})$
3: $J \leftarrow \frac{1}{2}(v^\intercal\mathbf{s}_m)^2$ (or $J \leftarrow \frac{1}{2}\|\mathbf{s}_m\|_2^2$)
4: $J \leftarrow J + \mathbf{v}^\intercal\nabla_\mathbf{x}\mathbf{s}_m\mathbf{v}$
5: **return** J

In practice, we can tune M to find the sweet spot between variance and computation. In our experiments, we find that typically $M = 1$ is often a good choice.

3.2 SLICED SCORE ESTIMATION

As mentioned in section 2.2, the task of score estimation is to predict $\nabla_\mathbf{x}\log q(\mathbf{x})$ at some test point $\mathbf{x}$, given a set of samples $\mathbf{x}_1^N \overset{\text{i.i.d.}}{\sim} q(\mathbf{x})$. Our sliced score matching objective $\hat{J}(\boldsymbol{\theta};\mathbf{x}_1^N,\mathbf{v}_{11}^{NM})$ is particularly suitable for this task since it depends only on the scores.

In practice, we propose to use a vector-valued deep neural network $\mathbf{h}(\mathbf{x};\boldsymbol{\theta}) : \mathbb{R}^D \to \mathbb{R}^D$ as our score model. Then, substituting $\mathbf{h}$ into $\hat{J}(\boldsymbol{\theta};\mathbf{x}_1^N,\mathbf{v}_{11}^{NM})$ for $\mathbf{s}_m$, we get

$$\frac{1}{N}\frac{1}{M}\sum_{i=1}^N\sum_{j=1}^M \mathbf{v}_{ij}^\intercal\nabla_\mathbf{x}\mathbf{h}(\mathbf{x}_i;\boldsymbol{\theta})\mathbf{v}_{ij} + \frac{1}{2}\left(\mathbf{v}_{ij}^\intercal\mathbf{h}(\mathbf{x}_i;\boldsymbol{\theta})\right)^2,$$

and we can optimize the objective to get $\hat{\boldsymbol{\theta}}$. Afterwards, $\mathbf{h}(\mathbf{x};\hat{\boldsymbol{\theta}})$ can be used as an approximation to $\nabla_\mathbf{x}\log q(\mathbf{x})$.[1]

---

[1]Note that $\mathbf{h}(\mathbf{x};\boldsymbol{\theta})$ may not correspond to the gradient of any scalar function. For $\mathbf{h}(\mathbf{x};\boldsymbol{\theta})$ to represent a gradient, one necessary condition is $\nabla_\mathbf{x} \times \mathbf{h}(\mathbf{x};\boldsymbol{\theta}) = 0$ for all $\mathbf{x}$, which may

By the same argument of integration by parts (*cf.*, Eq. (4), (5) and (6)), we have

$$\mathbb{E}_{p_\mathbf{v}}\mathbb{E}_{p_d}\left[\mathbf{v}^\intercal\nabla_\mathbf{x}\mathbf{h}(\mathbf{x};\boldsymbol{\theta})\mathbf{v} + \frac{1}{2}(\mathbf{v}^\intercal\mathbf{h}(\mathbf{x};\boldsymbol{\theta}))^2\right] =$$
$$\frac{1}{2}\mathbb{E}_{p_\mathbf{v}}\mathbb{E}_{p_d}[(\mathbf{v}^\intercal\mathbf{h}(\mathbf{x};\boldsymbol{\theta}) - \mathbf{v}^\intercal\nabla_\mathbf{x}\log q(\mathbf{x}))^2] + \mathrm{C},$$

which implies that minimizing $\hat{J}(\boldsymbol{\theta};\mathbf{x}_1^N,\mathbf{v}_{11}^{NM})$ with $\mathbf{s}_m(\mathbf{x};\boldsymbol{\theta})$ replaced by $\mathbf{h}(\mathbf{x};\boldsymbol{\theta})$ is approximately minimizing the average projected difference between $\mathbf{h}(\mathbf{x};\boldsymbol{\theta})$ and $\nabla_\mathbf{x}\log q(\mathbf{x})$. Hence, $\mathbf{h}(\mathbf{x};\hat{\boldsymbol{\theta}})$ should be close to $\nabla_\mathbf{x}\log q(\mathbf{x})$ and can serve as a score estimator.

4 ANALYSIS

In this section, we present several theoretical results to justify sliced score matching as a principled objective. We also discuss the connection of sliced score matching to other methods. For readability, we will defer rigorous statements of assumptions and theorems to the Appendix.

4.1 CONSISTENCY

One important question to ask for any statistical estimation objective is whether the estimated parameter is consistent under reasonable assumptions. Our results confirm that for any M, the objective $\hat{J}(\boldsymbol{\theta};\mathbf{x}_1^N,\mathbf{v}_{11}^{NM})$ is consistent under suitable assumptions as $N \to \infty$.

We need several standard assumptions to prove the results rigorously. Let p_m be the normalized density induced by our unnormalized model $\tilde{p}_m$. First, we assume Θ is compact (Assumption 6), and our model family $\{p_m(\mathbf{x};\boldsymbol{\theta}) : \boldsymbol{\theta} \in \Theta\}$ is well-specified and identifiable (Assumption 4). These are standard assumptions used for proving the consistency of MLE (van der Vaart, 1998). We also adopt the assumption in Hyvärinen (2005) that all densities are positive (Assumption 5). Finally, we assume that $p_m(\mathbf{x};\boldsymbol{\theta})$ has some Lipschitz properties (Assumption 7, which always holds if $\mathbf{s}_m(\mathbf{x};\boldsymbol{\theta})$ and $\nabla_\mathbf{x}\mathbf{s}_m(\mathbf{x};\boldsymbol{\theta})$ have uniformly bounded derivatives w.r.t. $\boldsymbol{\theta}$), and $p_\mathbf{v}$ has bounded higher-order moments (Assumption 2, true for all $p_\mathbf{v}$ considered in the experiments). Then, we can prove the consistency of $\hat{\boldsymbol{\theta}}_{N,M} \triangleq \arg\min_{\boldsymbol{\theta}\in\Theta}\hat{J}(\boldsymbol{\theta};\mathbf{x}_1^N,\mathbf{v}_{11}^{NM})$:

Theorem 2 (Consistency). *Assume the conditions of Theorem 1 are satisfied. Assume further that the assumptions discussed above hold. Let $\boldsymbol{\theta}^*$ be the true parameter of the data distribution. Then for every $M \in \mathbb{N}^+$,*

$$\hat{\boldsymbol{\theta}}_{N,M} \overset{p}{\to} \boldsymbol{\theta}^*, \quad N \to \infty.$$

---

not be satisfied by general networks. However, because Theorem 1 does not depend on the fact that $\mathbf{s}_m(\mathbf{x};\boldsymbol{\theta})$ is a gradient, we can still use the estimator in practice.

Sketch of proof. We first prove that $J(\boldsymbol{\theta}; p_{\mathbf{v}}) = 0 \Leftrightarrow \boldsymbol{\theta} = \boldsymbol{\theta}^*$ (Lemma 1 and Theorem 1). Then we prove the uniform convergence of $\hat{J}(\boldsymbol{\theta}; \mathbf{x}_1^N, \mathbf{v}_{11}^{NM})$ (Lemma 3), which holds regardless of M. These two facts lead to consistency. For a complete proof, see Appendix B.3. $\square$

Remark 1. *In Hyvärinen (2005), the authors only showed that $J(\boldsymbol{\theta}) = 0 \Leftrightarrow \boldsymbol{\theta} = \boldsymbol{\theta}^*$, which leads to "local consistency" of score matching. This is a weaker notion of consistency compared to our settings.*

4.2 ASYMPTOTIC NORMALITY

Asymptotic normality results can be very useful for approximate hypothesis testing and comparing different estimators. Below we show that $\hat{\boldsymbol{\theta}}_{N,M}$ is asymptotically normal when $N \to \infty$.

In addition to the assumptions in Section 4.1, we need an extra assumption to prove asymptotic normality. We require $p_m(\mathbf{x}; \boldsymbol{\theta})$ to have a stronger Lipschitz property (Assumption 9). The assumption holds if $\mathbf{s}_m(\mathbf{x}; \boldsymbol{\theta})$ and $\nabla_{\mathbf{x}} \mathbf{s}_m(\mathbf{x}; \boldsymbol{\theta})$, as functions of $\boldsymbol{\theta}$, have uniformly bounded third derivatives.

For simplicity, we denote $\nabla_{\mathbf{x}} h(\mathbf{x})|_{\mathbf{x}=\mathbf{x}'}$ as $\nabla_{\mathbf{x}} h(\mathbf{x}')$, where $h(\cdot)$ is an arbitrary function. In the following, we will only show the asymptotic normality result for a specific $p_{\mathbf{v}}$. More results can be found in Appendix B.4.

Theorem 3 (Asymptotic normality, special case). *Assume the assumptions discussed above hold. If $p_{\mathbf{v}}$ is the multivariate Rademacher distribution, we have*

$$\sqrt{N}(\hat{\boldsymbol{\theta}}_{N,M} - \boldsymbol{\theta}^*) \xrightarrow{d} \mathcal{N}(0, \Sigma),$$

where

$$\Sigma \triangleq [\nabla_{\boldsymbol{\theta}}^2 J(\boldsymbol{\theta}^*)]^{-1} \left(\sum_{1 \le i,j \le D} V_{ij} + \frac{2}{M} \sum_{1 \le i \ne j \le D} W_{ij} \right) \cdot [\nabla_{\boldsymbol{\theta}}^2 J(\boldsymbol{\theta}^*)]^{-1}. \quad (9)$$

Here D is the dimension of data; V_{ij} and W_{ij} are p.s.d matrices depending on $p_m(\mathbf{x}; \boldsymbol{\theta}^*)$, and their definitions can be found in Appendix B.4.

Sketch of proof. Once we get the consistency (Theorem 2), the rest closely follows the proof of asymptotic normality of MLE (van der Vaart, 1998). A rigorous proof can be found in Appendix B.4. $\square$

Remark 2. *As expected, larger M will lead to smaller asymptotic variance.*

Remark 3. *As far as we know, there is no published proof of asymptotic normality for score matching. However, by using the same techniques in our proofs, and*

under the same assumptions, we can conclude that the asymptotic variance of the score matching estimator is $[\nabla_{\boldsymbol{\theta}}^2 J(\boldsymbol{\theta}^*)]^{-1} \left(\sum_{ij} V_{ij} \right) [\nabla_{\boldsymbol{\theta}}^2 J(\boldsymbol{\theta}^*)]^{-1}$ (Corollary 1), which will always be smaller than sliced score matching with multivariate Rademacher projections. However, the gap reduces when M increases.

4.3 CONNECTION TO OTHER METHODS

Sliced score matching is widely connected to many other methods, and can be motivated from some different perspectives. Here we discuss a few of them.

Connection to NCE Noise contrastive estimation (NCE), proposed by Gutmann & Hyvärinen (2010), is another principle for training unnormalized statistical models. The method works by comparing $p_m(\mathbf{x}; \boldsymbol{\theta})$ with a noise distribution $p_n(\mathbf{x})$. We consider a special form of NCE which minimizes the following objective

$$-\mathbb{E}_{p_d}[\log h(\mathbf{x}; \boldsymbol{\theta})] - \mathbb{E}_{p_n}[\log(1 - h(\mathbf{x}; \boldsymbol{\theta}))], \quad (10)$$

where $h(\mathbf{x}; \boldsymbol{\theta}) \triangleq \frac{p_m(\mathbf{x}; \boldsymbol{\theta})}{p_m(\mathbf{x}; \boldsymbol{\theta}) + p_m(\mathbf{x}-\mathbf{v}; \boldsymbol{\theta})}$, and $p_n(\mathbf{x}) = p_d(\mathbf{x} + \mathbf{v})$. Assuming $\|\mathbf{v}\|_2$ to be small, Eq. (10) can be written as the following by Taylor expansion

$$\frac{1}{4} \mathbb{E}_{p_d} \left[\mathbf{v}^{\mathsf{T}} \nabla_{\mathbf{x}} \mathbf{s}_m(\mathbf{x}; \boldsymbol{\theta}) \mathbf{v} + \frac{1}{2} (\mathbf{s}_m(\mathbf{x}; \boldsymbol{\theta})^{\mathsf{T}} \mathbf{v})^2 \right] + 2 \log 2 + o(\|\mathbf{v}\|_2^2). \quad (11)$$

For derivation, see Proposition 1 in the appendix. A similar derivation can also be found in Gutmann & Hirayama (2011). As a result of (11), if we choose some $p_{\mathbf{v}}$ and take the expectation of (10) w.r.t. $p_{\mathbf{v}}$, the objective will be equivalent to sliced score matching whenever $\|\mathbf{v}\|_2 \approx 0$.

Connection to Hutchinson's Trick Hutchinson's trick (Hutchinson, 1990) is a stochastic algorithm to approximate $\operatorname{tr}(A)$ for any square matrix A. The idea is to choose a distribution of random vector $\mathbf{v}$ such that $\mathbb{E}_{p_{\mathbf{v}}}[\mathbf{v}\mathbf{v}^{\mathsf{T}}] = I$, and then we have $\operatorname{tr}(A) = \mathbb{E}_{p_{\mathbf{v}}}[\mathbf{v} A \mathbf{v}^{\mathsf{T}}]$. Hence, using Hutchinson's trick, we can replace $\operatorname{tr}(\nabla_{\mathbf{x}} \mathbf{s}_m(\mathbf{x}; \boldsymbol{\theta}))$ with $\mathbb{E}_{p_{\mathbf{v}}}[\mathbf{v}^{\mathsf{T}} \nabla_{\mathbf{x}} \mathbf{s}_m(\mathbf{x}; \boldsymbol{\theta}) \mathbf{v}]$ in the score matching objective $J(\boldsymbol{\theta})$. Then the finite sample objective of score matching becomes

$$\frac{1}{N} \sum_{i=1}^N \left(\frac{1}{M} \sum_{j=1}^M \mathbf{v}_{ij}^{\mathsf{T}} \nabla_{\mathbf{x}} \mathbf{s}_m(\mathbf{x}_i; \boldsymbol{\theta}) \mathbf{v}_{ij} \right) + \frac{1}{2} \|\mathbf{s}_m(\mathbf{x}_i; \boldsymbol{\theta})\|_2^2,$$

which is exactly the sliced score matching objective with variance reduction $\hat{J}_{\mathrm{vr}}(\boldsymbol{\theta}; \mathbf{x}_1^N, \mathbf{v}_{11}^{NM})$.

5   RELATED WORK

5.1   SCALABLE SCORE MATCHING

To the best of our knowledge, there are three existing methods that are able to scale up score matching to learning deep models on high dimensional data.

Denoising Score Matching   Vincent (2011) proposes denoising score matching, a variant of score matching that completely circumvents the Hessian. Specifically, consider a noise distribution $q_\sigma(\tilde{\mathbf{x}} \mid \mathbf{x})$, and let $q_\sigma(\tilde{\mathbf{x}}) = \int q_\sigma(\tilde{\mathbf{x}} \mid \mathbf{x}) p_d(\mathbf{x}) \mathrm{d}\mathbf{x}$. Denoising score matching applies the original score matching to the noise-corrupted data distribution $q_\sigma(\tilde{\mathbf{x}})$, and the objective can be proven to be equivalent to the following

$$\frac{1}{2}\mathbb{E}_{q_\sigma(\tilde{\mathbf{x}}|\mathbf{x})p_d(\mathbf{x})}[\|\mathbf{s}_m(\tilde{\mathbf{x}}; \boldsymbol{\theta}) - \nabla \log q_\sigma(\tilde{\mathbf{x}} \mid \mathbf{x})\|_2^2],$$

which can be estimated without computing the Hessian. Although denoising score matching is much faster than score matching, it has obvious drawbacks. First, it can only recover the noise corrupted data distribution. Furthermore, choosing the parameters of the noise distribution is highly non-trivial and in practice the performance can be very sensitive to q_σ, and people often have to use heuristics. For example, Saremi et al. (2018) proposes a heuristic of choosing σ based on Parzen windows.

Approximate Backpropagation   Kingma & LeCun (2010) proposes a backpropagation method to approximately compute the trace of the Hessian. Because the backpropagation of the full Hessian scales quadratically w.r.t. the layer size, the authors limit backpropagation only to the diagonal so that it has the same cost as the usual backpropagation for computing loss gradients. However, there are no theoretical guarantees for approximation errors. In fact, the authors only did experiments on networks with a single hidden layer, in which case the approximation is exact. Moreover, there is no direct support for the proposed approximate backpropagation method in modern automatic differentiation frameworks.

Curvature Propagation   Martens et al. (2012) estimates the trace term in score matching by applying curvature propagation to compute an unbiased, complex-valued estimator of the diagonal of the Hessian. The work claims that curvature propagation will have the smallest variance among a class of estimators, which includes the Hutchinson estimator. However, their proof incorrectly evaluates the pseudo-variance of the complex-valued estimator instead of the variance. In practice, curvature propagation can have large variance when the number of nodes in the network is large, because it introduces noise for each

node in the network. Finally, implementing curvature propagation also requires manually modifying the backpropagation code, handling complex numbers in neural networks, and will be inefficient for networks of more general structures, such as recurrent neural networks.

5.2   KERNEL SCORE ESTIMATORS

Two prior methods for score estimation are based on a generalized form of Stein's identity (Stein, 1981; Gorham & Mackey, 2017):

$$\mathbb{E}_q[\mathbf{h}(\mathbf{x})\nabla_\mathbf{x} \log q(\mathbf{x})^\mathsf{T} + \nabla_\mathbf{x}\mathbf{h}(\mathbf{x})] = \mathbf{0}, \qquad (12)$$

where $q(\mathbf{x})$ is a continuous differentiable density and $\mathbf{h}(\mathbf{x})$ is a function satisfying some regularity conditions. Li & Turner (2018) propose to set $\mathbf{h}(\mathbf{x})$ as the feature map of some kernel in the *Stein class* (Liu et al., 2016) of q, and solve a finite-sample version of (12) to obtain estimates of $\nabla_\mathbf{x} \log q(\mathbf{x})$ at the sample points. We refer to this method as *Stein* in the experiments. Shi et al. (2018) adopt a different approach but also exploit (12). They build their estimator by expanding $\nabla_\mathbf{x} \log q(\mathbf{x})$ as a spectral series of eigenfunctions and solve for the coefficients using (12). Compared to *Stein*, their method is argued to have theoretical guarantees and principled out-of-sample estimation at an unseen test point. We refer to their method as *Spectral* in the experiments.

6   EXPERIMENTS

Our experiments include two parts: (1) to test the effectiveness of SSM in learning deep models for density estimation, and (2) to test the ability of SSM in providing score estimates for applications such as VAEs with implicit encoders and WAEs. Unless specified explicitly, we choose $M = 1$ by default.

6.1   DENSITY ESTIMATION

We evaluate SSM and its variance-reduced version (SSM-VR) for density estimation and compare against score matching (SM) and its three scalable baselines: denoising score matching (DSM), approximate backpropagation (approx BP), and curvature propagation (CP). All SSM methods use the multivariate Rademacher distribution as $p_\mathbf{v}$. Our results demonstrate that: (1) SSM is comparable in performance to score matching, (2) SSM outperforms other computationally efficient approximations to score matching, and (3) unlike score matching, SSM scales effectively to high dimensional data.
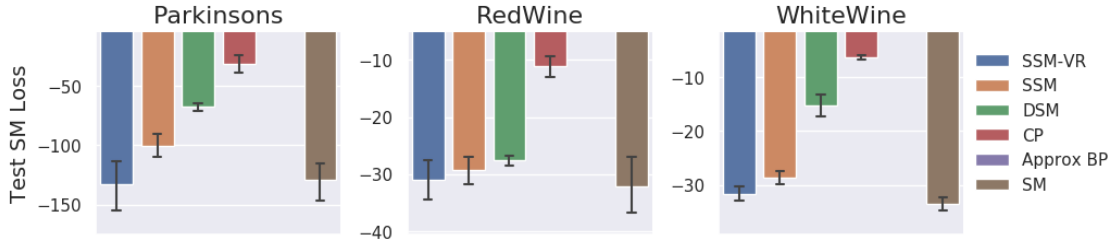
Figure 1: Score matching loss after training DKEF models on UCI datasets with different loss functions; lower is better. Results for approximate backprapogation are not shown because losses were larger than 10^9.
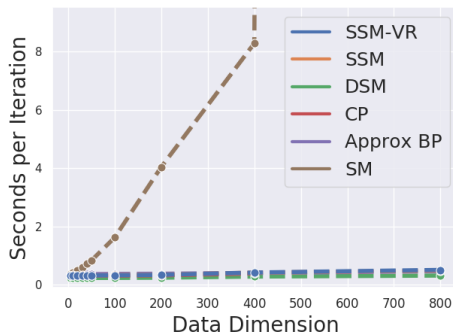

Figure 2: Score matching performance degrades linearly with the data dimension, while efficient approaches have relatively similar performance.

6.1.1 Deep Kernel Exponential Families

Model   Deep kernel exponential families (DKEF) are unnormalized density models trained using score matching (Wenliang et al., 2018). DKEFs parameterize the unnormalized log density as $\log \tilde{p}_f(\mathbf{x}) = f(\mathbf{x}) + \log q_0(\mathbf{x})$, where f is a mixture of Gaussian kernels evaluated at different inducing points: $f(\mathbf{x}) = \sum_{l=1}^{L} \alpha_l k(\mathbf{x}, \mathbf{z}_l)$. The kernel is defined on the feature space of a neural network, and the network parameters are trained along with the inducing points $\mathbf{z}_l$. Further details of the model, which is identical to that in Wenliang et al. (2018), are presented in Appendix C.1.

Setup   Following the settings of Wenliang et al. (2018), we trained models on three UCI datasets: Parkinsons, RedWine, and WhiteWine (Dua & Graff, 2017), and used their original code for score matching. To compute the trace term exactly, Wenliang et al. (2018)'s manual implementation of backpropagation takes over one thousand lines for a model that is four layers deep. For denoising score matching, the value of σ is chosen by grid search using the score matching loss on a validation dataset. All models are trained with 15 different random seeds and training is stopped when validation loss does not improve for 200 steps.

Results   Results in Fig. 1 demonstrate that SSM-VR performs comparably to score matching, when evaluated using the score matching loss on a held-out test set. We observe that variance reduction substantially improves the performance of SSM. In addition, SSM outperforms other computationally efficient approaches. DSM can perform comparably to SSM on RedWine. However, it is challenging to select σ for DSM. Models trained using σ from the heuristic in Saremi et al. (2018) are far from optimal (on both score matching losses and likelihoods), and extensive grid search is needed to find the best σ. CP performs substantially worse, which is likely because it injects noise for each node in the computation graph, and the amount of noise introduced is too large for a neural-network-based kernel evaluated at 200 inducing points, which supports our hypothesis that CP does not work effectively for deep models. Results for approximate backpropagation are omitted because the losses exceeded 10^9 on all datasets. This is because approx BP provides a biased estimate of the Hessian without any error guarantees. All the results are similar when evaluating with log-likelihoods (Appendix C.1).

Scalability to high dimensional data   We evaluate the computational efficiency of different losses on data of increasing dimensionality. We fit DKEF models to a multivariate standard normal in high dimensional spaces. The average running time per minibatch of 100 examples is reported in Fig. 2. Score matching performance degrades linearly with the dimension of the input data due to the computation of the Hessian, and creates out of memory errors for a 12GB GPU after the dimension increases beyond 400. SSM performs similarly to DSM, approx BP and CP, and they are all scalable to large dimensions.

6.1.2 Deep Flow Models

Setup   As a sanity check, we also evaluate SSM by training a NICE flow model (Dinh et al., 2015), whose likelihood is tractable and can be compared to ground truths obtained by MLE. The model we use has 20 hidden layers, and 1000 units per layer. Models are trained to fit

	Test SM Loss	Test LL
MLE	-579	**-791**
SSM-VR	**-8054**	-3355
SSM	-2428	-2039
DSM ($\sigma = 0.10$)	-3035	-4363
DSM ($\sigma = 1.74$)	-97	-8082
CP	-1694	-1517
Approx BP	-48	-2288

Table 1: Score matching losses and log-likelihoods for NICE models on MNIST. $\sigma = 0.1$ is by grid search and $\sigma = 1.74$ is from the heuristic of Saremi et al. (2018).

	VAE		WAE	
Latent Dim	8	32	8	32
ELBO	96.87	**89.06**	N/A	N/A
SSM	**95.50**	89.25 (**88.29**†)	**98.24**	**90.37**
Stein	96.71	91.84	99.05	91.70
Spectral	96.60	94.67	98.81	92.55

Table 2: Negative log-likelihoods on MNIST, estimated by AIS. †The result of SSM with $M = 100$, in which case SSM matches the computational cost of kernel methods, which used 100 samples for each data point.

	Iteration / Method	10k	40k	70k	100k
VAE	ELBO	**96.20**	73.70	69.42	66.32
	SSM	108.52	**70.28**	**66.52**	**62.50**
	Stein	126.60	118.87	120.51	126.76
	Spectral	131.90	125.04	128.36	133.93
WAE	SSM	84.11	**61.09**	**56.23**	**54.33**
	Stein	82.93	63.46	58.53	57.61
	Spectral	**82.30**	62.47	58.03	55.96

Table 3: FID scores of different methods versus number of training iterations on CelebA dataset.

MNIST handwritten digits, which are 784 dimensional images. Data are dequantized by adding uniform noise in the range $[-\frac{1}{512}, \frac{1}{512}]$, and transformed using a logit transformation, $\log(x) - \log(1 - x)$. We provide additional details in Appendix C.2.

Training with score matching is extremely computationally expensive in this case. Our SM implementation based on auto-differentiation takes around 7 hours to finish one epoch of training, and 12 GB GPU memory cannot hold a batch size larger than 24, so we do not include these results. Since NICE has tractable likelihoods, we also evaluate MLE as a surrogate objective for minimizing the score matching loss. Notably, likelihoods and score matching losses might be uncorrelated when the model is mis-specified, which is likely to be the case for a complex dataset like MNIST.

Results Score matching losses and log-likelihoods on the test dataset are reported in Tab. 1, where models are evaluated using the best checkpoint in terms of the score matching loss on a validation dataset over 100 epochs of training. SSM-VR greatly outperforms all the other methods on the score matching loss. DSM performs worse than SSM-VR, and σ is still hard to tune. Specifically, following the heuristic in Saremi et al. (2018) leads to $\sigma = 1.74$, which performed the worst (on both log-likelihood and SM loss) of the eight choices of σ in our grid search. Approx BP has more success on NICE than for training DKEF models. It is probably because the Hessians of hidden layers of NICE are closer to a diagonal matrix, which results in a smaller approximation error for approx BP. As in the DKEF experiments, CP performs worse. This is likely due to injecting noise to all hidden units, which will lead to large variance for a network as big as NICE. Unlike the DKEF experiments, we find that good log-likelihoods are less correlated with good score matching loss, probably due to model mis-specification.

6.2 SCORE ESTIMATION

We consider two typical tasks that require accurate score estimations: 1) training VAEs with an implicit encoder and 2) training Wasserstein Auto-Encoders. We show in both tasks SSM outperforms previous score estimators. Samples generated by various algorithms can be found in Appendix A.

6.2.1 VAE with Implicit Encoders

Background Consider a latent variable model $p(\mathbf{x}, \mathbf{z})$, where $\mathbf{x}$ and $\mathbf{z}$ denote observed and latent variables respectively. A variational auto-encoder (VAE) is composed of two parts: 1) an encoder $p_{\boldsymbol{\theta}}(\mathbf{x} \mid \mathbf{z})$ modeling the conditional distribution of $\mathbf{x}$ given $\mathbf{z}$; and a decoder $q_{\boldsymbol{\phi}}(\mathbf{z} \mid \mathbf{x})$ that approximates the posterior distribution of the latent variable. A VAE is typically trained by maximizing the following evidence lower bound (ELBO)

$$\mathbb{E}_{p_d}[\mathbb{E}_{q_{\boldsymbol{\phi}}(\mathbf{z}|\mathbf{x})} \log p_{\boldsymbol{\theta}}(\mathbf{x} \mid \mathbf{z})p(\mathbf{z}) - \mathbb{E}_{q_{\boldsymbol{\phi}}(\mathbf{z}|\mathbf{x})} \log q_{\boldsymbol{\phi}}(\mathbf{z} \mid \mathbf{x})],$$

where $p(\mathbf{z})$ denotes a pre-specified prior distribution. The expressive power of $q_{\boldsymbol{\phi}}(\mathbf{z} \mid \mathbf{x})$ is critical to the success of variational learning. Typically, $q_{\boldsymbol{\phi}}(\mathbf{z} \mid \mathbf{x})$ is chosen to be a simple distribution so that $H(q_{\boldsymbol{\phi}}) \triangleq -\mathbb{E}_{q_{\boldsymbol{\phi}}(\mathbf{z}|\mathbf{x})} \log q_{\boldsymbol{\phi}}(\mathbf{z} \mid \mathbf{x})$ is tractable. We call this traditional approach "ELBO" in the experiments. With score estimation techniques, we can directly compute $\nabla_{\boldsymbol{\phi}} H(q_{\boldsymbol{\phi}})$ for implicit distributions, which enables more flexible options for $q_{\boldsymbol{\phi}}$. We consider 3

score estimation techniques: sliced score matching (SSM), Stein (Li & Turner, 2018) and Spectral (Shi et al., 2018).

Given a data point $\mathbf{x}$, kernel score estimators need multiple samples from $q_\phi(\mathbf{z} \mid \mathbf{x})$ to estimate its score. On MNIST, we use 100 samples, as done in Shi et al. (2018). On CelebA, however, we can only take 20 samples due to GPU memory limitations. In contrast, SSM learns a score network $h(\mathbf{z} \mid \mathbf{x})$ along with $q_\phi(\mathbf{z} \mid \mathbf{x})$, which amortizes the cost of score estimation. Unless noted explicitly, we use one projection per data point ($M = 1$) for SSM, which is much more scalable to large networks.

Setup We consider VAE training on MNIST and CelebA (Liu et al., 2015). All images in CelebA are first cropped to a patch of 140×140 and then resized to 64×64. We report negative likelihoods on MNIST, as estimated by AIS (Neal, 2001) with 1000 intermediate distributions. We evaluate sample quality on CelebA with FID scores (Heusel et al., 2017). For fast AIS evaluation on MNIST, we use shallow fully-connected networks with 3 hidden layers. For CelebA experiments we use deep convolutional networks. The architectures of implicit encoders and score networks are straightforward modifications to the encoders of ELBO. More details are provided in Appendix C.3.

Results The negative likelihoods of different methods on MNIST are reported in the left part of Tab. 2. We note that SSM outperforms Stein and Spectral in all cases. When the latent dimension is 8, SSM outperforms ELBO, which indicates that the expressive power of implicit $q_\phi(\mathbf{z} \mid \mathbf{x})$ pays off. When the latent dimension is 32, the gaps between SSM and kernel methods are even larger, and the performance of SSM is still comparable to ELBO. Moreover, when $M = 100$ (matching the computation of kernel methods), SSM outperforms ELBO.

For CelebA, we provide FID scores of samples in the top part of Tab. 3. We observe that after 40k training iterations, SSM outperforms all other baselines. Kernel methods perform poorly in this case because only 20 samples per data point can be used due to limited amount of GPU memory. Early during training, SSM does not perform as well. Since the score network is trained along with the encoder and decoder, a moderate number of training steps is needed to give an accurate score estimation (and better learning of the VAE).

6.2.2 WAEs

Background WAE is another method to learn latent variable models, which generally produces better samples than VAEs. Similar to a VAE, it contains an encoder $q_\phi(\mathbf{z} \mid \mathbf{x})$ and a decoder $p_\theta(\mathbf{x} \mid \mathbf{z})$ and both can be

implicit distributions. Let $p(\mathbf{z})$ be a pre-defined prior distribution, and $q_\phi(\mathbf{z}) \triangleq \int q_\phi(\mathbf{z} \mid \mathbf{x}) p_d(\mathbf{x}) \mathrm{d}\mathbf{x}$ denote the aggregated posterior distribution. Using a metric function $c(\cdot, \cdot)$ and KL divergence between $q_\phi(\mathbf{z})$ and $p(\mathbf{z})$, WAE minimizes the following objective

$$\mathbb{E}_{p_d}[\mathbb{E}_{q_\phi(\mathbf{z}|\mathbf{x})}[c(\mathbf{x}, p_\theta(\mathbf{x} \mid \mathbf{z})) - \lambda \log p(\mathbf{z})]] - \lambda H(q_\phi(\mathbf{z})).$$

Here $\nabla_\phi H(q_\phi)$ can again be approximated by score estimators. Note that in this case kernel methods can work efficiently, as the samples from $q_\phi(\mathbf{z})$ can be collected by sampling one $\mathbf{z}$ for each $\mathbf{x}$ in a mini-batch. For SSM, we use a score network $h(\mathbf{z})$ and train it alongside $q_\phi(\mathbf{z} \mid \mathbf{x})$.

Setup The setup for WAE experiments is largely the same as VAE. The architectures are very similar to those used in the VAE experiments, and the only difference is that we made decoders implicit, as suggested in Tolstikhin et al. (2018). More details can be found in Appendix C.3.

Results The negative likelihoods on MNIST are provided in the right part of Tab. 2. SSM outperforms both kernel methods, and achieves a larger performance gap when the latent dimension is higher. The likelihoods are lower than the VAE results as the WAE objective does not directly maximize likelihoods.

We show FID scores for CelebA experiments in the bottom part of Tab. 3. As expected, kernel methods perform much better than before, because it is faster to sample from $q_\phi(\mathbf{z})$. The FID scores are generally lower than those in VAE experiments, which supports the forklore that WAEs generally obtain better samples. SSM outperforms both kernel methods when the number of iterations is more than 40k. This shows the advantages of training a deep, expressive score network compared to using a fixed kernel in score estimation tasks.

7 CONCLUSION

We propose sliced score matching, a scalable method for learning unnormalized statistical models and providing score estimates for implicit distributions. Compared to the original score matching and its variants, our estimator can scale to large-data scenarios, while remaining cheap to implement in modern auto-differentiation frameworks. Theoretically, our estimator is consistent and asymptotically normal under some regularity conditions. Experimental results demonstrate that our method outperforms competitors in learning deep energy-based models and provides more accurate estimates than kernel score estimators in training implicit VAEs and WAEs.

References

Abadi, M., Barham, P., Chen, J., Chen, Z., Davis, A., Dean, J., Devin, M., Ghemawat, S., Irving, G., Isard, M., et al. Tensorflow: A system for large-scale machine learning. In *12th {USENIX} Symposium on Operating Systems Design and Implementation ({OSDI} 16)*, pp. 265–283, 2016.

Adam, P., Soumith, C., Gregory, C., Edward, Y., Zachary, D., Zeming, L., Alban, D., Luca, A., and Adam, L. Automatic differentiation in pytorch. In *NIPS Autodiff Workshop*, 2017.

Canu, S. and Smola, A. Kernel methods and the exponential family. *Neurocomputing*, 69(7):714 – 720, 2006. ISSN 0925-2312. New Issues in Neurocomputing: 13th European Symposium on Artificial Neural Networks.

Dinh, L., Krueger, D., and Bengio, Y. NICE: Non-linear independent components estimation. *International Conference in Learning Representations Workshop Track*, 2015.

Dua, D. and Graff, C. UCI machine learning repository, 2017. URL http://archive.ics.uci.edu/ml.

Dudley, R. M. The sizes of compact subsets of hilbert space and continuity of Gaussian processes. *Journal of Functional Analysis*, 1(3):290–330, 1967.

Goodfellow, I., Pouget-Abadie, J., Mirza, M., Xu, B., Warde-Farley, D., Ozair, S., Courville, A., and Bengio, Y. Generative adversarial nets. In *Advances in Neural Information Processing Systems*, pp. 2672–2680, 2014.

Gorham, J. and Mackey, L. Measuring sample quality with kernels. In *Proceedings of the 34th International Conference on Machine Learning*, pp. 1292–1301, 2017.

Gutmann, M. and Hyvärinen, A. Noise-contrastive estimation: A new estimation principle for unnormalized statistical models. In *Proceedings of the Thirteenth International Conference on Artificial Intelligence and Statistics*, pp. 297–304, 2010.

Gutmann, M. U. and Hirayama, J.-i. Bregman divergence as general framework to estimate unnormalized statistical models. In *Proceedings of the Twenty-Seventh Conference on Uncertainty in Artificial Intelligence*, pp. 283–290. AUAI Press, 2011.

Heusel, M., Ramsauer, H., Unterthiner, T., Nessler, B., and Hochreiter, S. Gans trained by a two time-scale update rule converge to a local nash equilibrium. In *Advances in Neural Information Processing Systems*, pp. 6626–6637, 2017.

Huszár, F. Variational inference using implicit distributions. *arXiv preprint arXiv:1702.08235*, 2017.

Hutchinson, M. F. A stochastic estimator of the trace of the influence matrix for laplacian smoothing splines. *Communications in Statistics-Simulation and Computation*, 19(2):433–450, 1990.

Hyvärinen, A. Estimation of non-normalized statistical models by score matching. *Journal of Machine Learning Research*, 6(Apr):695–709, 2005.

Kingma, D. P. and LeCun, Y. Regularized estimation of image statistics by score matching. In *Advances in Neural Information Processing Systems*, pp. 1126–1134, 2010.

Kingma, D. P. and Welling, M. Auto-encoding variational bayes. *International Conference on Learning Representations*, 2014.

LeCun, Y., Chopra, S., Hadsell, R., Ranzato, M. A., and Huang, F. J. A tutorial on energy-based learning. In *Predicting structured data*. MIT Press, 2006.

Li, Y. and Turner, R. E. Gradient estimators for implicit models. In *International Conference on Learning Representations*, 2018.

Liu, Q., Lee, J., and Jordan, M. A kernelized Stein discrepancy for goodness-of-fit tests. In *Proceedings of The 33rd International Conference on Machine Learning*, pp. 276–284, 2016.

Liu, Z., Luo, P., Wang, X., and Tang, X. Deep learning face attributes in the wild. In *Proceedings of International Conference on Computer Vision (ICCV)*, 2015.

Martens, J., Sutskever, I., and Swersky, K. Estimating the hessian by back-propagating curvature. *Proceedings of the 29th International Conference on Machine Learning*, 2012.

Neal, R. M. Annealed importance sampling. *Statistics and computing*, 11(2):125–139, 2001.

Owen, A. B. *Monte Carlo theory, methods and examples*. 2013.

Rabin, J., Peyré, G., Delon, J., and Bernot, M. Wasserstein barycenter and its application to texture mixing. In Bruckstein, A. M., ter Haar Romeny, B. M., Bronstein, A. M., and Bronstein, M. M. (eds.), *Scale Space and Variational Methods in Computer Vision*, pp. 435–446, Berlin, Heidelberg, 2012. Springer Berlin Heidelberg. ISBN 978-3-642-24785-9.

Saremi, S., Mehrjou, A., Schölkopf, B., and Hyvärinen, A. Deep energy estimator networks. *arXiv preprint arXiv:1805.08306*, 2018.

Sasaki, H., Hyvärinen, A., and Sugiyama, M. Clustering via mode seeking by direct estimation of the gradient of a log-density. In *Joint European Conference on Machine Learning and Knowledge Discovery in Databases*, pp. 19–34. Springer, 2014.

Shi, J., Sun, S., and Zhu, J. A spectral approach to gradient estimation for implicit distributions. In *Proceedings of the 35th International Conference on Machine Learning*, pp. 4651–4660, 2018.

Sriperumbudur, B., Fukumizu, K., Gretton, A., Hyvärinen, A., and Kumar, R. Density estimation in infinite dimensional exponential families. *Journal of Machine Learning Research*, 18(57):1–59, 2017.

Stein, C. M. Estimation of the mean of a multivariate normal distribution. *The annals of Statistics*, pp. 1135–1151, 1981.

Strathmann, H., Sejdinovic, D., Livingstone, S., Szabo, Z., and Gretton, A. Gradient-free hamiltonian monte carlo with efficient kernel exponential families. In *Advances in Neural Information Processing Systems*, pp. 955–963, 2015.

Sun, S., Zhang, G., Shi, J., and Grosse, R. Functional variational Bayesian neural networks. In *International Conference on Learning Representations*, 2019.

Sutherland, D., Strathmann, H., Arbel, M., and Gretton, A. Efficient and principled score estimation with nyström kernel exponential families. In *Proceedings of the Twenty-First International Conference on Artificial Intelligence and Statistics*, pp. 652–660, 2018.

Tolstikhin, I., Bousquet, O., Gelly, S., and Schoelkopf, B. Wasserstein auto-encoders. In *International Conference on Learning Representations*, 2018.

Tran, D., Ranganath, R., and Blei, D. Hierarchical implicit models and likelihood-free variational inference. In *Advances in Neural Information Processing Systems*, pp. 5523–5533, 2017.

van der Vaart, A. W. *Asymptotic Statistics*. Cambridge Series in Statistical and Probabilistic Mathematics. Cambridge University Press, 1998. doi: 10.1017/CBO9780511802256.

Vincent, P. A connection between score matching and denoising autoencoders. *Neural computation*, 23(7):1661–1674, 2011.

Wenliang, L., Sutherland, D., Strathmann, H., and Gretton, A. Learning deep kernels for exponential family densities. *arXiv e-prints*, art. arXiv:1811.08357, Nov 2018.

A Samples

A.1 VAE WITH IMPLICIT ENCODERS

A.1.1 MNIST

	Latent Dim 8	Latent Dim 32
ELBO		
SSM		
Stein		
Spectral		

Table 4: VAE samples on MNIST.

A.1.2 CelebA

(a) ELBO

(b) SSM

(c) Stein

(d) Spectral

Table 5: VAE samples on CelebA.

A.2 WAE

A.2.1 MNIST

Table 6: WAE samples on MNIST.

A.2.2 CelebA

SSM

Stein

Spectral

Table 7: WAE samples on CelebA.

B PROOFS

B.1 NOTATIONS

Below we provide a summary of the most commonly used notations used in the proofs. First, we denote the data distribution as $p_d(\mathbf{x})$ and assume that the training/test data $\{\mathbf{x}_1, \mathbf{x}_2, \cdots, \mathbf{x}_N\}$ are i.i.d. samples of $p_d(\mathbf{x})$. The model is denoted as $p_m(\mathbf{x}; \boldsymbol{\theta})$, where $\boldsymbol{\theta}$ is restricted to a parameter space Θ. Note that $p_m(\mathbf{x}; \mathbf{v})$ can be an unnormalized energy-based model. We use $\mathbf{v}$ to represent a random vector with the same dimension of input $\mathbf{x}$. This vector $\mathbf{v}$ is often called the *projection vector*, and we use $p_\mathbf{v}$ to denote its distribution.

Next, we introduce several shorthand notations for quantities related to $p_m(\mathbf{x}; \boldsymbol{\theta})$ and $p_d(\mathbf{x})$. The log-likelihood $\log p_m(\mathbf{x}; \boldsymbol{\theta})$ and $\log p_d(\mathbf{x})$ are respectively denoted as $l_m(\mathbf{x}; \boldsymbol{\theta})$ and $l_d(\mathbf{x})$. The (Stein) score function $\nabla_\mathbf{x} \log p_m(\mathbf{x}; \boldsymbol{\theta})$ and $\nabla_\mathbf{x} \log p_d(\mathbf{x})$ are written as $\mathbf{s}_m(\mathbf{x}; \boldsymbol{\theta})$ and $\mathbf{s}_d(\mathbf{x})$, and finally the Hessian of $\log p_m(\mathbf{x}; \boldsymbol{\theta})$ w.r.t. $\mathbf{x}$ is denoted as $\nabla \mathbf{s}_m(\mathbf{x}; \boldsymbol{\theta})$.

We also adopt some convenient notations for collections. In particular, we use $\mathbf{x}_1^N$ to denote a collection of N vectors $\{\mathbf{x}_1, \mathbf{x}_2, \cdots, \mathbf{x}_N\}$ and use $\mathbf{v}_{11}^{NM}$ to denote $N \times M$ vectors $\{\mathbf{v}_{11}, \mathbf{v}_{12}, \cdots, \mathbf{v}_{1M}, \mathbf{v}_{21}, \mathbf{v}_{22}, \cdots, \mathbf{v}_{2M}, \cdots, \mathbf{v}_{N1}, \mathbf{v}_{N2}, \cdots, \mathbf{v}_{NM}\}$.

B.2 BASIC PROPERTIES

The following regularity conditions are needed for integration by parts and identifiability.

Assumption 1 (Regularity of score functions). *The model score function $\mathbf{s}_m(\mathbf{x})$ and data score function $\mathbf{s}_d(\mathbf{x})$ are both differentiable. They additionally satisfy $\mathbb{E}_{p_d}[\|\mathbf{s}_m(\mathbf{x})\|_2^2] < \infty$ and $\mathbb{E}_{p_d}[\|\mathbf{s}_d(\mathbf{x})\|_2^2] < \infty$.*

Assumption 2 (Regularity of projection vectors). *The projection vectors satisfy $\mathbb{E}_{p_\mathbf{v}}[\|\mathbf{v}\|_2^2] < \infty$, and $\mathbb{E}_{p_\mathbf{v}}[\mathbf{v}\mathbf{v}^\mathsf{T}] \succ 0$.*

Assumption 3 (Boundary conditions). *$\forall \boldsymbol{\theta} \in \Theta, \lim_{\|\mathbf{x}\| \to \infty} \mathbf{s}_m(\mathbf{x}; \boldsymbol{\theta}) p_d(\mathbf{x}) = 0$.*

Assumption 4 (Identifiability). *The model family $\{p_m(\mathbf{x}; \boldsymbol{\theta}) \mid \boldsymbol{\theta} \in \Theta\}$ is well-specified, i.e., $p_d(\mathbf{x}) = p_m(\mathbf{x}; \boldsymbol{\theta}^*)$. Furthermore, $p_m(\mathbf{x}; \boldsymbol{\theta}) \neq p_m(\mathbf{x}; \boldsymbol{\theta}^*)$ whenever $\boldsymbol{\theta} \neq \boldsymbol{\theta}^*$.*

Assumption 5 (Positiveness). *$p_m(\mathbf{x}; \boldsymbol{\theta}) > 0, \forall \boldsymbol{\theta} \in \Theta$ and $\forall \mathbf{x}$.*

Theorem 1. *Assume $\mathbf{s}_m(\mathbf{x}; \boldsymbol{\theta}), \mathbf{s}_d(\mathbf{x})$ and $p_\mathbf{v}$ satisfy some regularity conditions (Assumption 1, Assumption 2). Under proper boundary conditions (Assumption 3), we have*

$$L(\boldsymbol{\theta}; p_\mathbf{v}) \triangleq \frac{1}{2} \mathbb{E}_{p_\mathbf{v}} \mathbb{E}_{p_d} \left[(\mathbf{v}^\mathsf{T} \mathbf{s}_m(\mathbf{x}; \boldsymbol{\theta}) - \mathbf{v}^\mathsf{T} \mathbf{s}_d(\mathbf{x}))^2 \right] = \mathbb{E}_{p_\mathbf{v}} \mathbb{E}_{p_d} \left[\mathbf{v}^\mathsf{T} \nabla \mathbf{s}_m(\mathbf{x}; \boldsymbol{\theta}) \mathbf{v} + \frac{1}{2} \left(\mathbf{v}^\mathsf{T} \mathbf{s}_m(\mathbf{x}; \boldsymbol{\theta}) \right)^2 \right] + \text{const}, \quad (13)$$

where const *is a constant w.r.t. $\boldsymbol{\theta}$.*

Proof. The basic idea of this proof is similar to that of Theorem 1 in Hyvärinen (2005). First, note that $L(\boldsymbol{\theta}, p_\mathbf{v})$ can be expanded to

$$
\begin{aligned}
L(\boldsymbol{\theta}, p_\mathbf{v}) &= \frac{1}{2} \mathbb{E}_{p_\mathbf{v}} \mathbb{E}_{p_d} \left[(\mathbf{v}^\mathsf{T} \mathbf{s}_m(\mathbf{x}; \boldsymbol{\theta}) - \mathbf{v}^\mathsf{T} \mathbf{s}_d(\mathbf{x}))^2 \right] \\
&\overset{(i)}{=} \frac{1}{2} \mathbb{E}_{p_\mathbf{v}} \mathbb{E}_{p_d} [(\mathbf{v}^\mathsf{T} \mathbf{s}_m(\mathbf{x}; \boldsymbol{\theta}))^2 + (\mathbf{v}^\mathsf{T} \mathbf{s}_d(\mathbf{x}))^2 - 2(\mathbf{v}^\mathsf{T} \mathbf{s}_m(\mathbf{x}; \boldsymbol{\theta}))(\mathbf{v}^\mathsf{T} \mathbf{s}_d(\mathbf{x}))] \quad (14) \\
&= \mathbb{E}_{p_\mathbf{v}} \mathbb{E}_{p_d} \left[-(\mathbf{v}^\mathsf{T} \mathbf{s}_m(\mathbf{x}; \boldsymbol{\theta}))(\mathbf{v}^\mathsf{T} \mathbf{s}_d(\mathbf{x})) + \frac{1}{2} \left(\mathbf{v}^\mathsf{T} \mathbf{s}_m(\mathbf{x}; \boldsymbol{\theta}) \right)^2 \right] + \text{const}, \quad (15)
\end{aligned}
$$

where (i) is due to the assumptions of bounded expectations. We have absorbed the second term in the bracket of (14) into const since it does not depend on $\boldsymbol{\theta}$. Now what we need to prove is

$$-\mathbb{E}_{p_\mathbf{v}} \mathbb{E}_{p_d} [(\mathbf{v}^\mathsf{T} \mathbf{s}_m(\mathbf{x}; \boldsymbol{\theta}))(\mathbf{v}^\mathsf{T} \mathbf{s}_d(\mathbf{x}))] = \mathbb{E}_{p_\mathbf{v}} \mathbb{E}_{p_d} [\mathbf{v}^\mathsf{T} \nabla \mathbf{s}_m(\mathbf{x}; \boldsymbol{\theta}) \mathbf{v}]. \quad (16)$$

This can be shown by first observing that

$$-\mathbb{E}_{p_\mathbf{v}} \mathbb{E}_{p_d} [(\mathbf{v}^\mathsf{T} \mathbf{s}_m(\mathbf{x}; \boldsymbol{\theta}))(\mathbf{v}^\mathsf{T} \mathbf{s}_d(\mathbf{x}))]$$

$$= -\mathbb{E}_{p_{\mathbf{v}}} \int p_d(\mathbf{x})(\mathbf{v}^\mathsf{T} \mathbf{s}_m(\mathbf{x}; \boldsymbol{\theta}))(\mathbf{v}^\mathsf{T} \mathbf{s}_d(\mathbf{x}; \boldsymbol{\theta})) \mathrm{d}\mathbf{x}$$

$$= -\mathbb{E}_{p_{\mathbf{v}}} \int p_d(\mathbf{x})(\mathbf{v}^\mathsf{T} \nabla_{\mathbf{x}} \log p_m(\mathbf{x}; \boldsymbol{\theta}))(\mathbf{v}^\mathsf{T} \nabla_{\mathbf{x}} \log p_d(\mathbf{x})) \mathrm{d}\mathbf{x}$$

$$= -\mathbb{E}_{p_{\mathbf{v}}} \int (\mathbf{v}^\mathsf{T} \nabla_{\mathbf{x}} \log p_m(\mathbf{x}; \boldsymbol{\theta}))(\mathbf{v}^\mathsf{T} \nabla_{\mathbf{x}} p_d(\mathbf{x})) \mathrm{d}\mathbf{x}$$

$$= -\mathbb{E}_{p_{\mathbf{v}}} \sum_{i=1}^{D} \int (\mathbf{v}^\mathsf{T} \nabla_{\mathbf{x}} \log p_m(\mathbf{x}; \boldsymbol{\theta})) v_i \frac{\partial p_d(\mathbf{x})}{\partial x_i} \mathrm{d}\mathbf{x}, \tag{17}$$

where we assume $\mathbf{x} \in \mathbb{R}^D$. Then, applying multivariate integration by parts (*cf*., Lemma 4 in Hyvärinen (2005)), we obtain

$$\left| \mathbb{E}_{p_{\mathbf{v}}} \sum_{i=1}^{D} \int (\mathbf{v}^\mathsf{T} \mathbf{s}_m(\mathbf{x}; \boldsymbol{\theta})) v_i \frac{\partial p_d(\mathbf{x})}{\partial x_i} \mathrm{d}\mathbf{x} + \mathbb{E}_{p_{\mathbf{v}}} \sum_{i=1}^{D} \int v_i p_d(\mathbf{x}) \mathbf{v}^\mathsf{T} \frac{\partial \mathbf{s}_m(\mathbf{x}; \boldsymbol{\theta})}{\partial x_i} \mathrm{d}\mathbf{x} \right|$$

$$= \left| \mathbb{E}_{p_{\mathbf{v}}} \left[\sum_{i=1}^{D} \lim_{x_i \to \infty} (\mathbf{v}^\mathsf{T} \mathbf{s}_m(\mathbf{x}; \boldsymbol{\theta})) v_i p_d(\mathbf{x}) - \sum_{i=1}^{D} \lim_{x_i \to -\infty} (\mathbf{v}^\mathsf{T} \mathbf{s}_m(\mathbf{x}; \boldsymbol{\theta})) v_i p_d(\mathbf{x}) \right] \right|$$

$$\leq \sum_{i=1}^{D} \lim_{x_i \to \infty} \sum_{j=1}^{D} \mathbb{E}_{p_{\mathbf{v}}} |v_i v_j| |s_{m,j}(\mathbf{x}; \boldsymbol{\theta}) p_d(\mathbf{x})| + \sum_{i=1}^{D} \lim_{x_i \to -\infty} \sum_{j=1}^{D} \mathbb{E}_{p_{\mathbf{v}}} |v_i v_j| |s_{m,j}(\mathbf{x}; \boldsymbol{\theta}) p_d(\mathbf{x})|$$

$$\overset{(i)}{\leq} \sum_{i=1}^{D} \lim_{x_i \to \infty} \sum_{j=1}^{D} \sqrt{\mathbb{E}_{p_{\mathbf{v}}} v_i^2 \mathbb{E}_{p_{\mathbf{v}}} v_j^2} |s_{m,j}(\mathbf{x}; \boldsymbol{\theta}) p_d(\mathbf{x})| + \sum_{i=1}^{D} \lim_{x_i \to -\infty} \sum_{j=1}^{D} \sqrt{\mathbb{E}_{p_{\mathbf{v}}} v_i^2 \mathbb{E}_{p_{\mathbf{v}}} v_j^2} |s_{m,j}(\mathbf{x}; \boldsymbol{\theta}) p_d(\mathbf{x})|$$

$$\overset{(ii)}{=} 0,$$

where $s_{m,j}(\mathbf{x}; \boldsymbol{\theta})$ denotes the j-th component of $\mathbf{s}_m(\mathbf{x}; \boldsymbol{\theta})$. In the above derivation, (i) is due to Cauchy-Schwarz inequality and (ii) is from the assumption that $\mathbb{E}_{p_{\mathbf{v}}}[\|\mathbf{v}\|^2] < \infty$ and $s(\mathbf{x}; \boldsymbol{\theta}) p_d(\mathbf{x})$ vanishes at infinity.

Now returning to (17), we have

$$-\mathbb{E}_{p_{\mathbf{v}}} \sum_{i=1}^{D} \int (\mathbf{v}^\mathsf{T} \nabla_{\mathbf{x}} \log p_m(\mathbf{x}; \boldsymbol{\theta})) v_i \frac{\partial p_d(\mathbf{x})}{\partial x_i} \mathrm{d}\mathbf{x} = \mathbb{E}_{p_{\mathbf{v}}} \sum_{i=1}^{D} \int v_i p_d(\mathbf{x}) \mathbf{v}^\mathsf{T} \frac{\partial \mathbf{s}_m(\mathbf{x}; \boldsymbol{\theta})}{\partial x_i} \mathrm{d}\mathbf{x}$$

$$= \mathbb{E}_{p_{\mathbf{v}}} \int p_d(\mathbf{x}) \mathbf{v}^\mathsf{T} \nabla_{\mathbf{x}} \mathbf{s}_m(\mathbf{x}; \boldsymbol{\theta}) \mathbf{v} \mathrm{d}\mathbf{x},$$

which proves (16) and the proof is completed. $\qquad \square$

Lemma 1. *Assume our model family is well-specified and identifiable (Assumption 4). Assume further that the densities are all positive (Assumption 5). When $p_{\mathbf{v}}$ satisfies some regularity conditions (Assumption 2), we have*

$$L(\boldsymbol{\theta}; p_{\mathbf{v}}) = 0 \Leftrightarrow \boldsymbol{\theta} = \boldsymbol{\theta}^*.$$

Proof. First, since $p_d(\mathbf{x}) = p_m(\mathbf{x}; \boldsymbol{\theta}^*) > 0$, $L(\boldsymbol{\theta}; p_{\mathbf{v}}) = 0$ implies

$$\frac{1}{2} \mathbb{E}_{p_{\mathbf{v}}} (\mathbf{v}^\mathsf{T} (\mathbf{s}_m(\mathbf{x}; \boldsymbol{\theta}) - \mathbf{s}_d(\mathbf{x})))^2 = 0$$

$$\Leftrightarrow \mathbb{E}_{p_{\mathbf{v}}} \mathbf{v}^\mathsf{T} (\mathbf{s}_m(\mathbf{x}; \boldsymbol{\theta}) - \mathbf{s}_d(\mathbf{x}))(\mathbf{s}_m(\mathbf{x}; \boldsymbol{\theta}) - \mathbf{s}_d(\mathbf{x}))^\mathsf{T} \mathbf{v} = 0$$

$$\Leftrightarrow (\mathbf{s}_m(\mathbf{x}; \boldsymbol{\theta}) - \mathbf{s}_d(\mathbf{x}))^\mathsf{T} \mathbb{E}_{p_{\mathbf{v}}}[\mathbf{v}\mathbf{v}^\mathsf{T}] (\mathbf{s}_m(\mathbf{x}; \boldsymbol{\theta}) - \mathbf{s}_d(\mathbf{x})) = 0$$

$$\overset{(i)}{\Leftrightarrow} \mathbf{s}_m(\mathbf{x}; \boldsymbol{\theta}) - \mathbf{s}_d(\mathbf{x}) = 0$$

$$\Leftrightarrow \log p_m(\mathbf{x}; \boldsymbol{\theta}) = \log p_d(\mathbf{x}) + c$$

where (i) holds because $\mathbb{E}_{p_{\mathbf{v}}}[\mathbf{v}\mathbf{v}^\mathsf{T}]$ is positive definite. Because $p_m(\mathbf{x}; \boldsymbol{\theta})$ and $p_d(\mathbf{x})$ are normalized probability density functions, we have $p_m(\mathbf{x}; \boldsymbol{\theta}) = p_d(\mathbf{x})$. The identifiability assumption gives $\boldsymbol{\theta} = \boldsymbol{\theta}^*$. This concludes the left to right direction of the implication and the converse direction is trivial. $\qquad \square$

B.3 CONSISTENCY

In addition to the assumptions in Theorem 1 and Lemma 1, we need the following regularity conditions to prove the consistency of $\hat{\boldsymbol{\theta}}_{N,M} \triangleq \arg\min_{\boldsymbol{\theta} \in \Theta} \hat{J}(\boldsymbol{\theta}; \mathbf{x}_1^N, \mathbf{v}_{11}^{NM})$.

Assumption 6 (Compactness). *The parameter space Θ is compact.*

Assumption 7 (Lipschitz continuity). *Both $\nabla \mathbf{s}_m(\mathbf{x}; \boldsymbol{\theta})$ and $\mathbf{s}_m(\mathbf{x}; \boldsymbol{\theta}) \mathbf{s}_m(\mathbf{x}; \boldsymbol{\theta})^\intercal$ are Lipschitz continuous in terms of Frobenious norm, i.e., $\forall \boldsymbol{\theta}_1 \in \Theta, \boldsymbol{\theta}_2 \in \Theta$, $\|\nabla \mathbf{s}_m(\mathbf{x}; \boldsymbol{\theta}_1) - \nabla \mathbf{s}_m(\mathbf{x}; \boldsymbol{\theta}_2)\|_F \leq L_1(\mathbf{x}) \|\boldsymbol{\theta}_1 - \boldsymbol{\theta}_2\|_2$ and $\|\mathbf{s}_m(\mathbf{x}; \boldsymbol{\theta}_1) \mathbf{s}_m(\mathbf{x}; \boldsymbol{\theta}_1)^\intercal - \mathbf{s}_m(\mathbf{x}; \boldsymbol{\theta}_2) \mathbf{s}_m(\mathbf{x}; \boldsymbol{\theta}_2)^\intercal\|_F \leq L_2(\mathbf{x}) \|\boldsymbol{\theta}_1 - \boldsymbol{\theta}_2\|_2$. In addition, we require $\mathbb{E}_{p_d}[L_1^2(\mathbf{x})] < \infty$ and $\mathbb{E}_{p_d}[L_2^2(\mathbf{x})] < \infty$.*

Assumption 8 (Bounded moments of projection vectors). $\mathbb{E}_{p_\mathbf{v}}[\|\mathbf{v}\mathbf{v}^\intercal\|_F^2] < \infty$.

Lemma 2. *Suppose $\mathbf{s}_m(\mathbf{x}; \boldsymbol{\theta})$ is sufficiently smooth (Assumption 7) and $p_\mathbf{v}$ has bounded higher-order moments (Assumption 8). Let $f(\boldsymbol{\theta}; \mathbf{x}, \mathbf{v}) \triangleq \mathbf{v}^\intercal \nabla \mathbf{s}_m(\mathbf{x}; \boldsymbol{\theta}) \mathbf{v} + \frac{1}{2}(\mathbf{v}^\intercal \mathbf{s}_m(\mathbf{x}; \boldsymbol{\theta}))^2$. Then $f(\boldsymbol{\theta}; \mathbf{x}, \mathbf{v})$ is Lipschitz continuous with constant $L(\mathbf{x}, \mathbf{v})$ and $\mathbb{E}_{p_d, p_\mathbf{v}}[L^2(\mathbf{x}, \mathbf{v})] < \infty$.*

Proof. Let $A(\boldsymbol{\theta}) \triangleq \nabla \mathbf{s}_m(\mathbf{x}; \boldsymbol{\theta})$ and $B(\boldsymbol{\theta}) \triangleq \mathbf{s}_m(\mathbf{x}; \boldsymbol{\theta}) \mathbf{s}_m(\mathbf{x}; \boldsymbol{\theta})^\intercal$. Consider $\boldsymbol{\theta}_1 \in \Theta, \boldsymbol{\theta}_2 \in \Theta$ and let D be the dimension of $\mathbf{v}$, we have

$$|f(\boldsymbol{\theta}_1; \mathbf{x}, \mathbf{v}) - f(\boldsymbol{\theta}_2; \mathbf{x}, \mathbf{v})|$$

$$= \sum_{i=1}^D \sum_{j=1}^D \left[v_i v_j (A(\boldsymbol{\theta}_1)_{ij} - A(\boldsymbol{\theta}_2)_{ij}) + \frac{1}{2} v_i v_j (B(\boldsymbol{\theta}_1)_{ij} - B(\boldsymbol{\theta}_2)_{ij}) \right]$$

$$\overset{(i)}{\leq} \sqrt{\sum_{i=1}^D \sum_{j=1}^D v_i^2 v_j^2} \sqrt{\sum_{i=1}^D \sum_{j=1}^D \left[(A(\boldsymbol{\theta}_1)_{ij} - A(\boldsymbol{\theta}_2)_{ij}) + \frac{1}{2} (B(\boldsymbol{\theta}_1)_{ij} - B(\boldsymbol{\theta}_2)_{ij}) \right]^2}$$

$$\overset{(ii)}{\leq} \sqrt{\sum_{i=1}^D \sum_{j=1}^D v_i^2 v_j^2} \sqrt{\sum_{i=1}^D \sum_{j=1}^D 2(A(\boldsymbol{\theta}_1)_{ij} - A(\boldsymbol{\theta}_2)_{ij})^2 + \frac{1}{2}(B(\boldsymbol{\theta}_1)_{ij} - B(\boldsymbol{\theta}_2)_{ij})^2}$$

$$\overset{(iii)}{\leq} \sqrt{\sum_{i=1}^D \sum_{j=1}^D v_i^2 v_j^2} \sqrt{2 L_1^2(\mathbf{x}) \|\boldsymbol{\theta}_1 - \boldsymbol{\theta}_2\|_2^2 + \frac{1}{2} L_2^2(\mathbf{x}) \|\boldsymbol{\theta}_1 - \boldsymbol{\theta}_2\|_2^2}$$

$$= \sqrt{\sum_{i=1}^D \sum_{j=1}^D v_i^2 v_j^2} \sqrt{2 L_1^2(\mathbf{x}) + \frac{1}{2} L_2^2(\mathbf{x})} \|\boldsymbol{\theta}_1 - \boldsymbol{\theta}_2\|_2 \,,$$

where (i) is Cauchy-Schwarz inequality, (ii) is Jensen's inequality, and (iii) is due to Assumption 7. Now let

$$L(\mathbf{x}, \mathbf{v}) \triangleq \sqrt{\sum_{i=1}^D \sum_{j=1}^D v_i^2 v_j^2} \sqrt{2 L_1^2(\mathbf{x}) + \frac{1}{2} L_2^2(\mathbf{x})}.$$

Then

$$\mathbb{E}_{p_d, p_\mathbf{v}}[L^2(\mathbf{x}, \mathbf{v})] \overset{(i)}{=} \mathbb{E}_{p_\mathbf{v}}\left[\sum_{i=1}^D \sum_{j=1}^D v_i^2 v_j^2 \right] \mathbb{E}_{p_d}\left[2 L_1^2(\mathbf{x}) + \frac{1}{2} L_2^2(\mathbf{x}) \right]$$

$$\overset{(ii)}{<} \infty,$$

where (i) results from the independence of $\mathbf{v}, \mathbf{x}$, and (ii) is due to Assumption 8 and Assumption 7. $\qquad \square$

Lemma 3 (Uniform convergence of the expected error). *Under Assumption 6-8, we have*

$$\mathbb{E}_{p_\mathbf{v}, p_d}\left[\sup_{\boldsymbol{\theta} \in \Theta} \left| \hat{J}(\boldsymbol{\theta}; \mathbf{x}_1^N, \mathbf{v}_{11}^{NM}) - J(\boldsymbol{\theta}; p_\mathbf{v}) \right| \right] \leq O\left(\text{diam}(\Theta) \sqrt{\frac{D}{N}} \right) \tag{18}$$

where $\text{diam}(\cdot)$ denotes the diameter and D is the dimension of Θ.

Proof. The proof consists of 3 steps. First, we use the symmetrization trick to get rid of the inner expectation term $J(\boldsymbol{\theta}; p_{\mathbf{v}}) = \mathbb{E}_{p_{\mathbf{v}}, p_d}[\hat{J}(\boldsymbol{\theta}; \mathbf{x}_1^N, \mathbf{v}_{11}^{NM})]$. Second, we use chaining to get an upper bound that involves integration of the metric entropy. Finally, we upper bound the metric entropy to obtain the uniform convergence bound.

Step 1: From Jensen's inequality, we obtain

$$\mathbb{E}_{p_{\mathbf{v}}, p_d}\Big[\sup_{\boldsymbol{\theta} \in \Theta} \big| \hat{J}(\boldsymbol{\theta}; \mathbf{x}_1^N, \mathbf{v}_{11}^{NM}) - J(\boldsymbol{\theta}; p_{\mathbf{v}}) \big| \Big]$$

$$= \mathbb{E}_{p_{\mathbf{v}}, p_d}\Big[\sup_{\boldsymbol{\theta} \in \Theta} \big| \hat{J}(\boldsymbol{\theta}; \mathbf{x}_1^N, \mathbf{v}_{11}^{NM}) - \mathbb{E}_{p_{\mathbf{v}}, p_d}[\hat{J}(\boldsymbol{\theta}; \mathbf{x}_1^N, \mathbf{v}_{11}^{NM})] \big| \Big]$$

$$= \mathbb{E}_{p_{\mathbf{v}}, p_d}\Big[\sup_{\boldsymbol{\theta} \in \Theta} \big| \hat{J}(\boldsymbol{\theta}; \mathbf{x}_1^N, \mathbf{v}_{11}^{NM}) - \mathbb{E}_{p_{\mathbf{v}}, p_d}[\hat{J}(\boldsymbol{\theta}; \mathbf{x'}_1^N, \mathbf{v'}_{11}^{NM})] \big| \Big]$$

$$\leq \mathbb{E}_{p_{\mathbf{v}}, p_d}\Big[\sup_{\boldsymbol{\theta} \in \Theta} \big| \hat{J}(\boldsymbol{\theta}; \mathbf{x}_1^N, \mathbf{v}_{11}^{NM}) - \hat{J}(\boldsymbol{\theta}; \mathbf{x'}_1^N, \mathbf{v'}_{11}^{NM}) \big| \Big],$$

where $\mathbf{x'}_1^N, \mathbf{v'}_{11}^{NM}$ are independent copies of $\mathbf{x}_1^N$ and $\mathbf{v}_{11}^{NM}$. Let $\{\epsilon_i\}_{i=1}^N$ be a set of independent Rademacher random variables, we have

$$\mathbb{E}_{p_{\mathbf{v}}, p_d}\Big[\sup_{\boldsymbol{\theta} \in \Theta} \big| \hat{J}(\boldsymbol{\theta}; \mathbf{x}_1^N, \mathbf{v}_{11}^{NM}) - \hat{J}(\boldsymbol{\theta}; \mathbf{x'}_1^N, \mathbf{v'}_{11}^{NM}) \big| \Big]$$

$$= \mathbb{E}_{p_{\mathbf{v}}, p_d}\Big[\sup_{\boldsymbol{\theta} \in \Theta} \frac{1}{N} \frac{1}{M} \Big| \sum_{i=1}^N \sum_{j=1}^M \underbrace{\mathbf{v}_{ij}^{\mathsf{T}} \nabla \mathbf{s}_m(\mathbf{x}_i; \boldsymbol{\theta}) \mathbf{v}_{ij} + \frac{1}{2} \big(\mathbf{v}_{ij}^{\mathsf{T}} \mathbf{s}_m(\mathbf{x}_i; \boldsymbol{\theta}) \big)^2}_{\triangleq f(\boldsymbol{\theta}; \mathbf{x}_i, \mathbf{v}_{ij})} - \underbrace{\Big[\mathbf{v'}_{ij}^{\mathsf{T}} \nabla \mathbf{s}_m(\mathbf{x}'_i; \boldsymbol{\theta}) \mathbf{v'}_{ij} + \frac{1}{2} \big(\mathbf{v'}_{ij}^{\mathsf{T}} \mathbf{s}_m(\mathbf{x}'_i; \boldsymbol{\theta}) \big)^2 \Big]}_{\triangleq f(\boldsymbol{\theta}; \mathbf{x}'_i, \mathbf{v'}_{ij})} \Big| \Big]$$

$$= \mathbb{E}_{p_{\mathbf{v}}, p_d}\Big[\sup_{\boldsymbol{\theta} \in \Theta} \frac{1}{N} \frac{1}{M} \Big| \sum_{i=1}^N \sum_{j=1}^M f(\boldsymbol{\theta}; \mathbf{x}_i, \mathbf{v}_{ij}) - f(\boldsymbol{\theta}; \mathbf{x}'_i, \mathbf{v'}_{ij}) \Big| \Big]$$

$$\overset{(i)}{=} \mathbb{E}\Big[\sup_{\boldsymbol{\theta} \in \Theta} \frac{1}{N} \frac{1}{M} \Big| \sum_{i=1}^N \sum_{j=1}^M \epsilon_i (f(\boldsymbol{\theta}; \mathbf{x}_i, \mathbf{v}_{ij}) - f(\boldsymbol{\theta}; \mathbf{x}'_i, \mathbf{v'}_{ij})) \Big| \Big]$$

$$\overset{(ii)}{\leq} \mathbb{E}\Big[\sup_{\boldsymbol{\theta} \in \Theta} \frac{1}{N} \frac{1}{M} \Big| \sum_{i=1}^N \sum_{j=1}^M \epsilon_i f(\boldsymbol{\theta}; \mathbf{x}_i, \mathbf{v}_{ij}) \Big| \Big] + \mathbb{E}\Big[\sup_{\boldsymbol{\theta} \in \Theta} \frac{1}{N} \frac{1}{M} \Big| \sum_{i=1}^N \sum_{j=1}^M \epsilon_i f(\boldsymbol{\theta}; \mathbf{x}'_i, \mathbf{v'}_{ij}) \Big| \Big]$$

$$= 2\mathbb{E}\Big[\sup_{\boldsymbol{\theta} \in \Theta} \frac{1}{N} \frac{1}{M} \Big| \sum_{i=1}^N \sum_{j=1}^M \epsilon_i f(\boldsymbol{\theta}; \mathbf{x}_i, \mathbf{v}_{ij}) \Big| \Big], \tag{19}$$

where (i) is because the quantity is symmetric about 0 in distribution, and (ii) is due to Jensen's inequality.

Step 2: First note that given $\mathbf{x}_i, \mathbf{v}_{ij}, \frac{\epsilon_i}{M} \sum_{j=1}^M f(\boldsymbol{\theta}; \mathbf{x}_i, \mathbf{v}_{ij})$ is a zero-mean sub-Gaussian process w.r.t. $\boldsymbol{\theta}$. This can be observed from

$$\mathbb{E}_{\epsilon_i} \Big[e^{\lambda \frac{\epsilon_i}{M} \sum_{j=1}^M [f(\boldsymbol{\theta}_1; \mathbf{x}_i, \mathbf{v}_{ij}) - f(\boldsymbol{\theta}_2; \mathbf{x}_i, \mathbf{v}_{ij})]} \Big]$$

$$\overset{(i)}{\leq} \exp\Big\{ \frac{\lambda^2}{2M^2} \Big(\sum_{j=1}^M [f(\boldsymbol{\theta}_1; \mathbf{x}_i, \mathbf{v}_{ij}) - f(\boldsymbol{\theta}_2; \mathbf{x}_i, \mathbf{v}_{ij})] \Big)^2 \Big\}$$

$$\overset{(ii)}{\leq} \exp\Big\{ \frac{\lambda^2}{2M^2} M \sum_{j=1}^M [f(\boldsymbol{\theta}_1; \mathbf{x}_i, \mathbf{v}_{ij}) - f(\boldsymbol{\theta}_2; \mathbf{x}_i, \mathbf{v}_{ij})]^2 \Big\}$$

$$\overset{(iii)}{\leq} \exp\Big\{ \frac{\lambda^2}{2M} \sum_{j=1}^M L^2(\mathbf{x}_i, \mathbf{v}_{ij}) \|\boldsymbol{\theta}_1 - \boldsymbol{\theta}_2\|^2 \Big\},$$

where (i) holds because ϵ_i is a 1-sub-Gaussian random variable, (ii) is from Cauchy-Schwarz inequality and (iii) is due to Lemma 2. As a result, $\frac{1}{N} \frac{1}{M} \sum_{i=1}^N \sum_{j=1}^M \epsilon_i f(\boldsymbol{\theta}; \mathbf{x}_i, \mathbf{v}_{ij})$ is a zero-mean sub-Gaussian random process with

metric

$$d(\boldsymbol{\theta}_1, \boldsymbol{\theta}_2) = \frac{1}{\sqrt{N}} \sqrt{\frac{1}{NM} \sum_{i=1}^{N} \sum_{j=1}^{M} L^2(\mathbf{x}_i, \mathbf{v}_{ij})} \|\boldsymbol{\theta}_1 - \boldsymbol{\theta}_2\|.$$

Since Θ is compact, the diameter of Θ with respect to the Euclidean norm $\|\cdot\|_2$ is finite and we denote it as $\mathrm{diam}(\Theta) < \infty$. Then, Dudley's entropy integral (Dudley, 1967) gives

$$\mathbb{E}\left[\sup_{\boldsymbol{\theta} \in \Theta} \left| \frac{1}{N} \frac{1}{M} \sum_{i=1}^{N} \sum_{j=1}^{M} \epsilon_i f(\boldsymbol{\theta}; \mathbf{x}_i, \mathbf{v}_{ij}) \right| \right] \leq O(1) \mathbb{E}\left[\int_0^{\frac{1}{\sqrt{N}} \sqrt{\frac{1}{NM} \sum_{i=1}^{N} \sum_{j=1}^{M} L^2(\mathbf{x}_i, \mathbf{v}_{ij})} \mathrm{diam}(\Theta)} \sqrt{\log N(\Theta, d, \epsilon)} \mathrm{d}\epsilon \right].$$
$$(20)$$

Here $\log N(\Theta, d, \epsilon)$ is the metric entropy of Θ with metric $d(\boldsymbol{\theta}_1, \boldsymbol{\theta}_2) = \frac{1}{\sqrt{N}} \sqrt{\frac{1}{NM} \sum_{i=1}^{N} \sum_{j=1}^{M} L^2(\mathbf{x}_i, \mathbf{v}_{ij})} \|\boldsymbol{\theta}_1 - \boldsymbol{\theta}_2\|_2$ and size ϵ.

Step 3: When the dimension of $\boldsymbol{\theta} \in \Theta$ is D, it is known that the ϵ-covering number of Θ with Euclidean distance is

$$N(\Theta, \|\cdot\|, \epsilon) \leq \left(1 + \frac{\mathrm{diam}(\Theta)}{\epsilon}\right)^D.$$

Therefore, $N(\Theta, d, \epsilon)$ can be bounded by

$$N(\Theta, d, \epsilon) \leq \left(1 + \sqrt{\frac{1}{NM} \sum_{i=1}^{N} \sum_{j=1}^{M} L^2(\mathbf{x}_i, \mathbf{v}_{ij})} \frac{\mathrm{diam}(\Theta)}{\sqrt{N}\epsilon}\right)^D.$$

Hence, the metric integral can be bounded

$$\int_0^{\frac{1}{\sqrt{N}} \sqrt{\frac{1}{NM} \sum_{i=1}^{N} \sum_{j=1}^{M} L^2(\mathbf{x}_i, \mathbf{v}_{ij})} \mathrm{diam}(\Theta)} \sqrt{\log N(\Theta, d, \epsilon)} \mathrm{d}\epsilon$$

$$\leq \int_0^{\frac{1}{\sqrt{N}} \sqrt{\frac{1}{NM} \sum_{i=1}^{N} \sum_{j=1}^{M} L^2(\mathbf{x}_i, \mathbf{v}_{ij})} \mathrm{diam}(\Theta)} \sqrt{D \log \left(1 + \sqrt{\frac{1}{NM} \sum_{i=1}^{N} \sum_{j=1}^{M} L^2(\mathbf{x}_i, \mathbf{v}_{ij})} \frac{\mathrm{diam}(\Theta)}{\sqrt{N}\epsilon}\right)} \mathrm{d}\epsilon$$

$$\leq \int_0^{\frac{1}{\sqrt{N}} \sqrt{\frac{1}{NM} \sum_{i=1}^{N} \sum_{j=1}^{M} L^2(\mathbf{x}_i, \mathbf{v}_{ij})} \mathrm{diam}(\Theta)} \sqrt{\sqrt{\frac{1}{NM} \sum_{i=1}^{N} \sum_{j=1}^{M} L^2(\mathbf{x}_i, \mathbf{v}_{ij})} \frac{D \, \mathrm{diam}(\Theta)}{\sqrt{N}\epsilon}} \mathrm{d}\epsilon$$

$$= 2 \sqrt{\frac{1}{NM} \sum_{i=1}^{N} \sum_{j=1}^{M} L^2(\mathbf{x}_i, \mathbf{v}_{ij})} \sqrt{\frac{D}{N}} \mathrm{diam}(\Theta) \qquad (21)$$

Finally, combining (19), (20) and (21) gives us

$$\mathbb{E}_{p_{\mathbf{v}}, p_d}\left[\sup_{\boldsymbol{\theta} \in \Theta} \left| \hat{J}(\boldsymbol{\theta}; \mathbf{x}_1^N, \mathbf{v}_{11}^{NM}) - J(\boldsymbol{\theta}; p_{\mathbf{v}}) \right| \right]$$

$$\leq 4 O(1) \mathbb{E}_{p_{\mathbf{v}}, p_d}\left[\sqrt{\frac{1}{NM} \sum_{i=1}^{N} \sum_{j=1}^{M} L^2(\mathbf{x}_i, \mathbf{v}_{ij})} \sqrt{\frac{D}{N}} \mathrm{diam}(\Theta) \right]$$

$$\overset{(i)}{\leq} O(1) \sqrt{\frac{D}{N}} \mathrm{diam}(\Theta) \sqrt{\mathbb{E}_{p_{\mathbf{v}}, p_d}\left[\frac{1}{NM} \sum_{i=1}^{N} \sum_{j=1}^{M} L^2(\mathbf{x}_i, \mathbf{v}_{ij}) \right]}$$

$$\overset{(ii)}{\leq} O(1)\operatorname{diam}(\Theta)\sqrt{\frac{D}{N}},$$

where (i) is due to Jensen's inequality and (ii) results from $\mathbb{E}[L^2(\mathbf{x},\mathbf{v})] < \infty$, and the compactness of Θ guarantees that the bound is finite. $\qquad\square$

Theorem 2. *Suppose all the previous assumptions hold (Assumption 1-Assumption 8). Assume further the conditions of Theorem 1 and Lemma 1 are satisfied. Let $\boldsymbol{\theta}^*$ be the true parameter of the data distribution, and $\hat{\boldsymbol{\theta}}_{N,M}$ be the empirical estimator defined by*

$$\hat{\boldsymbol{\theta}}_{N,M} \triangleq \arg\min_{\boldsymbol{\theta}\in\Theta} \hat{J}(\boldsymbol{\theta};\mathbf{x}_1^N,\mathbf{v}_{11}^{NM})$$

Then, $\hat{\boldsymbol{\theta}}_{N,M}$ is consistent, meaning that

$$\hat{\boldsymbol{\theta}}_{N,M} \overset{p}{\to} \boldsymbol{\theta}^*$$

as $N \to \infty$.

Proof. Note that Theorem 1 and 1 together imply that $\boldsymbol{\theta}^* = \arg\min_{\boldsymbol{\theta}\in\Theta} J(\boldsymbol{\theta};p_{\mathbf{v}})$. Then, we will show $J(\hat{\boldsymbol{\theta}}_{N,M};p_{\mathbf{v}}) \overset{p}{\to} J(\boldsymbol{\theta}^*;p_{\mathbf{v}})$ when $N \to \infty$. This can be done by noticing

$$\begin{aligned}
J(\hat{\boldsymbol{\theta}}_{N,M};p_{\mathbf{v}}) - J(\boldsymbol{\theta}^*;p_{\mathbf{v}}) =& J(\hat{\boldsymbol{\theta}}_{N,M};p_{\mathbf{v}}) - \hat{J}(\hat{\boldsymbol{\theta}}_{N,M};\mathbf{x}_1^N,\mathbf{v}_{11}^{NM}) + \hat{J}(\hat{\boldsymbol{\theta}}_{N,M};\mathbf{x}_1^N,\mathbf{v}_{11}^{NM}) - \hat{J}(\boldsymbol{\theta}^*;\mathbf{x}_1^N,\mathbf{v}_{11}^{NM}) \\
& + \hat{J}(\boldsymbol{\theta}^*;\mathbf{x}_1^N,\mathbf{v}_{11}^{NM}) - J(\boldsymbol{\theta}^*;p_{\mathbf{v}}) \\
\leq& \sup_{\boldsymbol{\theta}\in\Theta} |\hat{J}(\boldsymbol{\theta};\mathbf{x}_1^N,\mathbf{v}_{11}^{NM}) - J(\boldsymbol{\theta};p_{\mathbf{v}})| + |\hat{J}(\boldsymbol{\theta}^*;\mathbf{x}_1^N,\mathbf{v}_{11}^{NM}) - J(\boldsymbol{\theta}^*;p_{\mathbf{v}})| \\
\leq& 2\sup_{\boldsymbol{\theta}\in\Theta} |\hat{J}(\boldsymbol{\theta};\mathbf{x}_1^N,\mathbf{v}_{11}^{NM}) - J(\boldsymbol{\theta};p_{\mathbf{v}})| \qquad\qquad (22)
\end{aligned}$$

We can easily conclude that (22) is $o_p(1)$ with the help of Lemma 3, because

$$P\left(\sup_{\boldsymbol{\theta}\in\Theta} |\hat{J}(\boldsymbol{\theta};\mathbf{x}_1^N,\mathbf{v}_{11}^{NM}) - J(\boldsymbol{\theta};p_{\mathbf{v}})| > t\right) \leq \mathbb{E}\left[\sup_{\boldsymbol{\theta}\in\Theta} |\hat{J}(\boldsymbol{\theta};\mathbf{x}_1^N,\mathbf{v}_{11}^{NM}) - J(\boldsymbol{\theta};p_{\mathbf{v}})|\right]/t \leq O(1)\sqrt{\frac{1}{Nt^2}} \to 0,$$

as $N \to \infty$. From Lemma 1 we also have $L(\hat{\boldsymbol{\theta}}_{N,M};p_{\mathbf{v}}) - L(\boldsymbol{\theta}^*;p_{\mathbf{v}}) > 0$ if $\hat{\boldsymbol{\theta}}_{N,M} \neq \boldsymbol{\theta}$. As shown by Theorem 1, this is the same as $J(\hat{\boldsymbol{\theta}}_{N,M};p_{\mathbf{v}}) - J(\boldsymbol{\theta}^*;p_{\mathbf{v}}) > 0$ if $\hat{\boldsymbol{\theta}}_{N,M} \neq \boldsymbol{\theta}$. Therefore (22) = $o_p(1)$ gives $J(\hat{\boldsymbol{\theta}}_{N,M};p_{\mathbf{v}}) \overset{p}{\to} J(\boldsymbol{\theta}^*;p_{\mathbf{v}})$.

Next, we show $\hat{\boldsymbol{\theta}}_{N,M} \overset{p}{\to} \boldsymbol{\theta}^*$. This can be inferred from $J(\hat{\boldsymbol{\theta}}_{N,M};p_{\mathbf{v}}) \overset{p}{\to} J(\boldsymbol{\theta}^*;p_{\mathbf{v}})$ because $J(\boldsymbol{\theta};p_{\mathbf{v}})$ is continuous (Assumption 7) and Θ is compact (Assumption 6). The proof is reductio ad absurdum. Specifically, assume that $\hat{\boldsymbol{\theta}}_{N,M} \overset{p}{\not\to} \boldsymbol{\theta}^*$. We know $\exists \epsilon > 0, \delta > 0, \forall K > 0, \exists N > K, M > 0$ such that $P(\|\hat{\boldsymbol{\theta}}_{N,M} - \boldsymbol{\theta}^*\| \geq \epsilon) \geq \delta$. Note that $J(\boldsymbol{\theta};p_{\mathbf{v}}) = \mathbb{E}[f(\boldsymbol{\theta};\mathbf{x},\mathbf{v})]$, $f(\boldsymbol{\theta};\mathbf{x},\mathbf{v})$ is Lipschitz continuous and $\mathbb{E}[L(\boldsymbol{\theta};\mathbf{x},\mathbf{v})] \leq \sqrt{\mathbb{E}[L^2(\boldsymbol{\theta};\mathbf{x},\mathbf{v})]} < \infty$. This implies that $J(\boldsymbol{\theta};p_{\mathbf{v}})$ is continuous w.r.t. $\boldsymbol{\theta}$. Since Θ is compact and $J(\boldsymbol{\theta};p_{\mathbf{v}})$ is continuous, we can define a compact set $\mathcal{S}_\epsilon \triangleq \{\boldsymbol{\theta}\in\Theta | \|\boldsymbol{\theta} - \boldsymbol{\theta}^*\| \geq \epsilon\}$ and let $\boldsymbol{\theta}_{\mathcal{S}_\epsilon} \triangleq \arg\min_{\boldsymbol{\theta}\in\mathcal{S}_\epsilon} J(\boldsymbol{\theta};p_{\mathbf{v}})$. Observe that

$$\begin{aligned}
p(J(\hat{\boldsymbol{\theta}}_{N,M};p_{\mathbf{v}}) \geq J(\boldsymbol{\theta}_{\mathcal{S}_\epsilon};p_{\mathbf{v}})) &= p(|J(\hat{\boldsymbol{\theta}}_{N,M};p_{\mathbf{v}}) - J(\boldsymbol{\theta}^*;p_{\mathbf{v}})| \geq J(\boldsymbol{\theta}_{\mathcal{S}_\epsilon};p_{\mathbf{v}}) - J(\boldsymbol{\theta}^*;p_{\mathbf{v}})) \\
&\geq p(\|\hat{\boldsymbol{\theta}}_{N,M} - \boldsymbol{\theta}^*\| \geq \epsilon) \geq \delta.
\end{aligned}$$

However, the fact that $p(|J(\hat{\boldsymbol{\theta}}_{N,M};p_{\mathbf{v}}) - J(\boldsymbol{\theta}^*;p_{\mathbf{v}})| \geq J(\boldsymbol{\theta}_{\mathcal{S}_\epsilon};p_{\mathbf{v}}) - J(\boldsymbol{\theta}^*;p_{\mathbf{v}})) \geq \delta$ holds for arbitrarily large N contradicts $J(\hat{\boldsymbol{\theta}}_{N,M};p_{\mathbf{v}}) \overset{p}{\to} J(\boldsymbol{\theta}^*;p_{\mathbf{v}})$. $\qquad\square$

B.4 ASYMPTOTIC NORMALITY

Notations To simplify notations we use $\partial_i\partial_j h(\cdot) \triangleq (\nabla_{\mathbf{x}}^2 h(\cdot))_{ij}$, $\partial_i h(\cdot) \triangleq (\nabla_{\mathbf{x}} h(\cdot))_i$, and denote $\nabla_{\mathbf{x}} h(\mathbf{x})|_{\mathbf{x}=\mathbf{x}'}$ as $\nabla_{\mathbf{x}} h(\mathbf{x}')$. Here $h(\cdot)$ denotes some arbitrary function. Let $l_m \triangleq \log p_m(\mathbf{x};\boldsymbol{\theta})$, $l_m(\mathbf{x};\boldsymbol{\theta}) \triangleq \log p_m(\mathbf{x};\boldsymbol{\theta})$ and further adopt the following notations

$$f(\boldsymbol{\theta};\mathbf{x},\mathbf{v}) \triangleq \mathbf{v}^\mathsf{T}\nabla\mathbf{s}_m(\mathbf{x};\boldsymbol{\theta})\mathbf{v} + \frac{1}{2}(\mathbf{v}^\mathsf{T}\mathbf{s}_m(\mathbf{x};\boldsymbol{\theta}))^2$$

$$f(\boldsymbol{\theta};\mathbf{x},\mathbf{v}_1^M) \triangleq \frac{1}{M}\sum_{j=1}^M f(\boldsymbol{\theta};\mathbf{x},\mathbf{v}_j) = \frac{1}{M}\sum_{j=1}^M \mathbf{v}_j^\mathsf{T}\nabla\mathbf{s}_m(\mathbf{x};\boldsymbol{\theta})\mathbf{v}_j + \frac{1}{2}(\mathbf{v}_j^\mathsf{T}\mathbf{s}_m(\mathbf{x};\boldsymbol{\theta}))^2$$

$$f(\boldsymbol{\theta};\mathbf{x}) \triangleq \mathrm{tr}(\nabla\mathbf{s}_m(\mathbf{x};\boldsymbol{\theta})) + \frac{1}{2}\|\mathbf{s}_m(\mathbf{x};\boldsymbol{\theta})\|_2^2$$

$$\Sigma_{ij} \triangleq (\mathbb{E}_{p_\mathbf{v}}[\mathbf{v}\mathbf{v}^\mathsf{T}])_{ij}$$

$$\mathfrak{S}_{ijpq} \triangleq \mathbb{E}_{p_\mathbf{v}}[v_i v_j v_p v_q]$$

$$\mathfrak{V}_{ijpq} \triangleq \mathbb{E}_{p_d}\left[\left(\nabla_{\boldsymbol{\theta}}\partial_i\partial_j l_m + \frac{1}{2}\nabla_{\boldsymbol{\theta}}(\partial_i l_m \partial_j l_m)\right)\left(\nabla_{\boldsymbol{\theta}}\partial_p\partial_q l_m + \frac{1}{2}\nabla_{\boldsymbol{\theta}}(\partial_p l_m \partial_q l_m)\right)^\mathsf{T}\right]\bigg|_{\boldsymbol{\theta}=\boldsymbol{\theta}^*}$$

$$V_{ij} \triangleq \mathfrak{V}_{iijj}$$

$$W_{ij} \triangleq \mathfrak{V}_{ijij}$$

For the proof of asymptotic normality we need the following extra assumptions.

Assumption 9 (Lipschitz smoothness on second derivatives). *For $\boldsymbol{\theta}_1$, $\boldsymbol{\theta}_2$ near $\boldsymbol{\theta}^*$, and $\forall i,j$,*

$$\left\|\nabla_{\boldsymbol{\theta}}^2\partial_i\partial_j l_m(\mathbf{x};\boldsymbol{\theta}_1) - \nabla_{\boldsymbol{\theta}}^2\partial_i\partial_j l_m(\mathbf{x};\boldsymbol{\theta}_2)\right\|_F \le M_{ij}(\mathbf{x})\|\boldsymbol{\theta}_1-\boldsymbol{\theta}_2\|_2$$

$$\left\|\nabla_{\boldsymbol{\theta}}^2\partial_i l_m(\mathbf{x};\boldsymbol{\theta}_1)\partial_j l_m(\mathbf{x};\boldsymbol{\theta}_1) - \nabla_{\boldsymbol{\theta}}^2\partial_i l_m(\mathbf{x};\boldsymbol{\theta}_2)\partial_j l_m(\mathbf{x};\boldsymbol{\theta}_2)\right\|_F \le N_{ij}(\mathbf{x})\|\boldsymbol{\theta}_1-\boldsymbol{\theta}_2\|_2$$

and

$$\mathbb{E}_{p_d}[M_{ij}^2(\mathbf{x})] < \infty, \quad \mathbb{E}_{p_d}[N_{ij}^2(\mathbf{x})] < \infty, \quad \forall i,j.$$

Lemma 4. *Suppose $l_m(\mathbf{x};\boldsymbol{\theta})$ is sufficiently smooth (Assumption 9) and $p_\mathbf{v}$ has bounded moments (Assumption 2 and Assumption 8). Let $\nabla_{\boldsymbol{\theta}}^2 f(\boldsymbol{\theta};\mathbf{x},\mathbf{v}_1^M) \triangleq \frac{1}{M}\sum_{i=1}^M \nabla_{\boldsymbol{\theta}}^2\mathbf{v}_i^\mathsf{T}\nabla\mathbf{s}_m(\mathbf{x};\boldsymbol{\theta})\mathbf{v}_i + \frac{1}{2}\nabla_{\boldsymbol{\theta}}^2(\mathbf{v}_i^\mathsf{T}\mathbf{s}_m(\mathbf{x};\boldsymbol{\theta}))^2$. Then $\nabla_{\boldsymbol{\theta}}^2 f(\boldsymbol{\theta};\mathbf{x},\mathbf{v})$ is Lipschitz continuous, i.e., for $\boldsymbol{\theta}_1$ and $\boldsymbol{\theta}_2$ close to $\boldsymbol{\theta}^*$, there exists a Lipschitz constant $L(\mathbf{x},\mathbf{v}_1^M)$ such that*

$$\left\|\nabla_{\boldsymbol{\theta}}^2 f(\boldsymbol{\theta}_1;\mathbf{x},\mathbf{v}_1^M) - \nabla_{\boldsymbol{\theta}}^2 f(\boldsymbol{\theta}_2;\mathbf{x},\mathbf{v}_1^M)\right\|_F \le L(\mathbf{x},\mathbf{v}_1^M)\|\boldsymbol{\theta}_1-\boldsymbol{\theta}_2\|_2,$$

and $\mathbb{E}_{p_d,p_\mathbf{v}}[L^2(\mathbf{x},\mathbf{v}_1^M)] < \infty$.

Proof. First, we write out $\nabla_{\boldsymbol{\theta}}^2 f(\boldsymbol{\theta}_1;\mathbf{x},\mathbf{v}_1^M) - \nabla_{\boldsymbol{\theta}}^2 f(\boldsymbol{\theta}_2;\mathbf{x},\mathbf{v}_1^M)$ according to the definitions. Let $A_{ij}(\boldsymbol{\theta}) \triangleq \nabla_{\boldsymbol{\theta}}^2\partial_i\partial_j l_m(\mathbf{x};\boldsymbol{\theta})$ and $B_{ij}(\boldsymbol{\theta}) \triangleq \nabla_{\boldsymbol{\theta}}^2\partial_i l_m(\mathbf{x};\boldsymbol{\theta})\partial_j l_m(\mathbf{x};\boldsymbol{\theta})$. Then,

$$\nabla_{\boldsymbol{\theta}}^2 f(\boldsymbol{\theta}_1;\mathbf{x},\mathbf{v}_1^M) - \nabla_{\boldsymbol{\theta}}^2 f(\boldsymbol{\theta}_2;\mathbf{x},\mathbf{v}_1^M) = \frac{1}{M}\sum_{i,j,k} v_{k,i} v_{k,j}\left[A_{ij}(\boldsymbol{\theta}_1) - A_{ij}(\boldsymbol{\theta}_2) + \frac{1}{2}(B_{ij}(\boldsymbol{\theta}_1) - B_{ij}(\boldsymbol{\theta}_2))\right].$$

Then, Cauchy-Schwarz and Jensen's inequality give

$$\left\|\nabla_{\boldsymbol{\theta}}^2 f(\boldsymbol{\theta}_1;\mathbf{x},\mathbf{v}_1^M) - \nabla_{\boldsymbol{\theta}}^2 f(\boldsymbol{\theta}_2;\mathbf{x},\mathbf{v}_1^M)\right\|_F^2$$

$$= \sum_{l,m}\left(\frac{1}{M}\sum_{i,j,k} v_{k,i} v_{k,j}\left[A_{ij}(\boldsymbol{\theta}_1)_{lm} - A_{ij}(\boldsymbol{\theta}_2)_{lm} + \frac{1}{2}(B_{ij}(\boldsymbol{\theta}_1)_{lm} - B_{ij}(\boldsymbol{\theta}_2))_{lm}\right]\right)^2$$

$$\le \sum_{l,m}\left(\frac{1}{M}\sqrt{\sum_{i,j}\left(\sum_k v_{k,i} v_{k,j}\right)^2}\cdot\sqrt{\sum_{i,j}\left[A_{ij}(\boldsymbol{\theta}_1)_{lm} - A_{ij}(\boldsymbol{\theta}_2)_{lm} + \frac{1}{2}(B_{ij}(\boldsymbol{\theta}_1)_{lm} - B_{ij}(\boldsymbol{\theta}_2))_{lm}\right]^2}\right)^2$$

$$\le \sum_{l,m}\frac{1}{M^2}\left(\sum_{i,j}\left(\sum_k v_{k,i} v_{k,j}\right)^2\right)\left(\sum_{i,j}\left(2\left[A_{ij}(\boldsymbol{\theta}_1)_{lm} - A_{ij}(\boldsymbol{\theta}_2)_{lm}\right]^2 + \frac{1}{2}\left[(B_{ij}(\boldsymbol{\theta}_1)_{lm} - B_{ij}(\boldsymbol{\theta}_2))_{lm}\right]^2\right)\right)$$

$$= \frac{1}{M^2}\left(\sum_{i,j}\left(\sum_k v_{k,i} v_{k,j}\right)^2\right)\left(\sum_{i,j}\left(\sum_{l,m} 2\left[A_{ij}(\boldsymbol{\theta}_1)_{lm} - A_{ij}(\boldsymbol{\theta}_2)_{lm}\right]^2 + \sum_{l,m}\frac{1}{2}\left[(B_{ij}(\boldsymbol{\theta}_1)_{lm} - B_{ij}(\boldsymbol{\theta}_2))_{lm}\right]^2\right)\right)$$

$$= \frac{1}{M^2} \left(\sum_{i,j,p,q} v_{p,i} v_{p,j} v_{q,i} v_{q,j} \right) \left(\sum_{i,j} \left(2 \left\| A_{ij}(\boldsymbol{\theta}_1) - A_{ij}(\boldsymbol{\theta}_2) \right\|_F^2 + \frac{1}{2} \left\| V_{ij}(\boldsymbol{\theta}_1) - V_{ij}(\boldsymbol{\theta}_2) \right\|_F^2 \right) \right)$$

$$\leq \underbrace{\frac{1}{M^2} \left(\sum_{i,j,p,q} v_{p,i} v_{p,j} v_{q,i} v_{q,j} \right) \left(\sum_{i,j} \left(2 M_{ij}^2 + \frac{1}{2} N_{ij}^2 \right) \right)}_{\triangleq L^2(\mathbf{x}, \mathbf{v}_1^M)} \left\| \boldsymbol{\theta}_1 - \boldsymbol{\theta}_2 \right\|_2^2$$

Next, we bound the expectation

$$\mathbb{E}_{p_d, p_\mathbf{v}}[L^2(\mathbf{x}, \mathbf{v}_1^M)] = \frac{1}{M^2} \mathbb{E}_{p_\mathbf{v}} \left[\sum_{i,j,p,q} v_{p,i} v_{p,j} v_{q,i} v_{q,j} \right] \mathbb{E}_{p_d} \left[\sum_{ij} 2 M_{ij}^2(\mathbf{x}) + \frac{1}{2} N_{ij}^2(\mathbf{x}) \right]$$

$$\overset{(i)}{\leq} O(1) \mathbb{E}_{p_\mathbf{v}} \left[\sum_{i,j,p,q} v_{p,i} v_{p,j} v_{q,i} v_{q,j} \right]$$

$$= O(1) \left(\sum_{ij} M(M-1) \mathbb{E}_{p_\mathbf{v}}[v_i v_j]^2 + M \mathbb{E}_{p_\mathbf{v}}[(v_i v_j)^2] \right)$$

$$= O(1) \left(M(M-1) \left\| \mathbb{E}_{p_\mathbf{v}}[\mathbf{v}\mathbf{v}^\mathsf{T}] \right\|_F^2 + M \mathbb{E}_{p_\mathbf{v}}[\| \mathbf{v}\mathbf{v}^\mathsf{T} \|_F^2] \right)$$

$$\overset{(ii)}{\leq} O(1) \left(M(M-1) \mathbb{E}_{p_\mathbf{v}}[\| \mathbf{v}\mathbf{v}^\mathsf{T} \|_F^2] + M \mathbb{E}_{p_\mathbf{v}}[\| \mathbf{v}\mathbf{v}^\mathsf{T} \|_F^2] \right) \overset{(iii)}{<} \infty,$$

where (i) is due to Assumption 9, (ii) is Jensen's, and (iii) is because of Assumption 2 and 8. $\qquad \square$

Lemma 5. *Assume that conditions in Theorem 1 and Lemma 1 hold, and $p_\mathbf{v}$ has bounded higher-order moments (Assumption 8). Then*

$$\mathrm{Var}_{p_d, p_\mathbf{v}} \left[\nabla_{\boldsymbol{\theta}} f(\boldsymbol{\theta}^*; \mathbf{x}, \mathbf{v}_1^M) \right] = \sum_{i,j,p,q} \left[\left(1 - \frac{1}{M} \right) \Sigma_{ij} \Sigma_{pq} + \frac{1}{M} \mathfrak{S}_{ijpq} \right] \mathfrak{V}_{ijpq}, \tag{23}$$

where $\nabla_{\boldsymbol{\theta}} f(\boldsymbol{\theta}^*; \mathbf{x}, \mathbf{v}_1^M) = \nabla_{\boldsymbol{\theta}} f(\boldsymbol{\theta}; \mathbf{x}, \mathbf{v}_1^M)\big|_{\boldsymbol{\theta} = \boldsymbol{\theta}^*}$

In particular, if $p_\mathbf{v} \sim \mathcal{N}(0, I)$, we have

$$\mathrm{Var}_{p_d, p_\mathbf{v}} \left[\nabla_{\boldsymbol{\theta}} f(\boldsymbol{\theta}^*; \mathbf{x}, \mathbf{v}_1^M) \right] = \sum_{ij} V_{ij} + \frac{2}{M} \sum_i V_{ii} + \frac{2}{M} \sum_{i \neq j} W_{ij}.$$

If $p_\mathbf{v}$ is the distribution of multivariate Rademacher random variables, we have

$$\mathrm{Var}_{p_d, p_\mathbf{v}} \left[\nabla_{\boldsymbol{\theta}} f(\boldsymbol{\theta}^*; \mathbf{x}, \mathbf{v}_1^M) \right] = \sum_{ij} V_{ij} + \frac{2}{M} \sum_{i \neq j} W_{ij}.$$

Proof. Since $\boldsymbol{\theta}^*$ is the true parameter of the data distribution, we have

$$\mathbb{E}_{p_d, p_\mathbf{v}}[\nabla_{\boldsymbol{\theta}} f(\boldsymbol{\theta}^*; \mathbf{x}, \mathbf{v}_1^M)] = \nabla_{\boldsymbol{\theta}} \mathbb{E}_{p_d, p_\mathbf{v}}[f(\boldsymbol{\theta}^*; \mathbf{x}, \mathbf{v}_1^M)] = \nabla_{\boldsymbol{\theta}} J(\boldsymbol{\theta}^*; p_\mathbf{v}) = 0.$$

Therefore, (23) can be expanded as

$$\mathrm{Var}_{p_d, p_\mathbf{v}} \left[\nabla_{\boldsymbol{\theta}} f(\boldsymbol{\theta}^*; \mathbf{x}, \mathbf{v}_1^M) \right]$$

$$= \mathbb{E}_{p_d, p_\mathbf{v}} \left[\nabla_{\boldsymbol{\theta}} f(\boldsymbol{\theta}^*; \mathbf{x}, \mathbf{v}_1^M) \nabla_{\boldsymbol{\theta}} f(\boldsymbol{\theta}^*; \mathbf{x}, \mathbf{v}_1^M)^\mathsf{T} \right]$$

$$= \mathbb{E} \left[\sum_{i,j,p,q} \left(\frac{1}{M^2} \sum_{k,l} v_{k,i} v_{k,j} v_{l,p} v_{l,q} \right) \left(\nabla_{\boldsymbol{\theta}} \partial_i \partial_j l_m + \frac{1}{2} \nabla_{\boldsymbol{\theta}} (\partial_i l_m \partial_j l_m) \right) \left(\nabla_{\boldsymbol{\theta}} \partial_p \partial_q l_m + \frac{1}{2} \nabla_{\boldsymbol{\theta}} (\partial_p l_m \partial_q l_m) \right)^\mathsf{T} \right]$$

$$= \sum_{i,j,p,q} \underbrace{\mathbb{E} \left[\frac{1}{M^2} \sum_{k,l} v_{k,i} v_{k,j} v_{l,p} v_{l,q} \right]}_{\triangleq E_1} \underbrace{\mathbb{E} \left[\left(\nabla_{\boldsymbol{\theta}} \partial_i \partial_j l_m + \frac{1}{2} \nabla_{\boldsymbol{\theta}} (\partial_i l_m \partial_j l_m) \right) \left(\nabla_{\boldsymbol{\theta}} \partial_p \partial_q l_m + \frac{1}{2} \nabla_{\boldsymbol{\theta}} (\partial_p l_m \partial_q l_m) \right)^\mathsf{T} \right]}_{\mathfrak{V}_{ijpq}}.$$

Continuing on E_1, we have that

$$E_1 = \frac{1}{M^2} \sum_{k \neq l} \mathbb{E}[v_{k,i}v_{k,j}]\mathbb{E}[v_{l,p}v_{l,q}] + \frac{1}{M^2} \sum_k \mathbb{E}[v_{k,i}v_{k,j}v_{k,p}v_{k,q}]$$

$$= \left(1 - \frac{1}{M}\right)\Sigma_{ij}\Sigma_{pq} + \frac{1}{M}\mathfrak{S}_{ijpq},$$

which leads to (23). Note that Assumption 2 guarantees that $|\Sigma_{ij}| < \infty$ and Assumption 8 ensures $|\mathfrak{S}_{ijpq}| < \infty$.

If $p_{\mathbf{v}} \sim \mathcal{N}(0, I)$, $\mathfrak{S}$ and Σ have the following simpler forms

$$\Sigma_{ij} = \delta_{ij}$$

$$\mathfrak{S}_{ijpq} = \begin{cases} 3, & i = j = p = q \\ 1, & i = j \neq p = q \text{ or } i = p \neq j = q \text{ or } i = q \neq j = p \\ 0, & \text{otherwise} \end{cases} .$$

Then, if we assume that the second derivatives of l_m are continuous, we have $\partial_i \partial_j l_m = \partial_j \partial_i l_m$, and the variance (23) can also be simplified to

$$\text{Var}_{p_d, p_{\mathbf{v}}}\left[\nabla_{\boldsymbol{\theta}} f(\boldsymbol{\theta}^*; \mathbf{x}, \mathbf{v}_1^M)\right] = \sum_{i \neq j} V_{ij} + \frac{M+2}{M} \sum_i V_{ii} + \frac{2}{M} \sum_{i \neq j} W_{ij} = \sum_{ij} V_{ij} + \frac{2}{M} \sum_i V_{ii} + \frac{2}{M} \sum_{i \neq j} W_{ij}.$$

Similarly, if $p_{\mathbf{v}} \sim \mathcal{U}(\{\pm 1\}^D)$, (23) has the simplified form

$$\text{Var}_{p_d, p_{\mathbf{v}}}\left[\nabla_{\boldsymbol{\theta}} f(\boldsymbol{\theta}^*; \mathbf{x}, \mathbf{v}_1^M)\right] = \sum_{ij} V_{ij} + \frac{2}{M} \sum_{i \neq j} W_{ij}.$$

$\square$

Theorem 3. *With the notations and assumptions in Lemma 4, Lemma 5 and Theorem 2, we have*

$$\sqrt{N}(\hat{\boldsymbol{\theta}}_{N,M} - \boldsymbol{\theta}^*) \xrightarrow{d}$$

$$\mathcal{N}\left(0, \left(\nabla_{\boldsymbol{\theta}}^2 J(\boldsymbol{\theta}^*; p_{\mathbf{v}})\right)^{-1}\left(\sum_{i,j,p,q}\left[\left(1 - \frac{1}{M}\right)\Sigma_{ij}\Sigma_{pq} + \frac{1}{M}\mathfrak{S}_{ijpq}\right]\mathfrak{V}_{ijpq}\right)\left(\nabla_{\boldsymbol{\theta}}^2 J(\boldsymbol{\theta}^*; p_{\mathbf{v}})\right)^{-1}\right).$$

In particular, if $p_{\mathbf{v}} \sim \mathcal{N}(0, I)$, then the asymptotic variance is

$$\left(\nabla_{\boldsymbol{\theta}}^2 J(\boldsymbol{\theta}^*)\right)^{-1}\left(\sum_{ij} V_{ij} + \frac{2}{M} \sum_i V_{ii} + \frac{2}{M} \sum_{i \neq j} W_{ij}\right)\left(\nabla_{\boldsymbol{\theta}}^2 J(\boldsymbol{\theta}^*)\right)^{-1}.$$

If $p_{\mathbf{v}}$ is the distribution of multivariate Rademacher random variables, the asymptotic variance is

$$\left(\nabla_{\boldsymbol{\theta}}^2 J(\boldsymbol{\theta}^*)\right)^{-1}\left(\sum_{ij} V_{ij} + \frac{2}{M} \sum_{i \neq j} W_{ij}\right)\left(\nabla_{\boldsymbol{\theta}}^2 J(\boldsymbol{\theta}^*)\right)^{-1}.$$

Proof. To simplify notations, we use $P_N h(\mathbf{x}) \triangleq \frac{1}{N}\sum_{i=1}^N h(\mathbf{x}_i, \cdot)$, where $h(\mathbf{x}, \cdot)$ is some arbitrary function. For example, $\hat{J}(\boldsymbol{\theta}; \mathbf{x}_1^N, \mathbf{v}_{11}^{NM})$ can be written as $P_N f(\boldsymbol{\theta}; \mathbf{x}, \mathbf{v}_1^M)$. By Taylor expansion, we can approximate $P_N \nabla_{\boldsymbol{\theta}} f(\hat{\boldsymbol{\theta}}_{N,M}; \mathbf{x}, \mathbf{v}_1^M)$ around $\boldsymbol{\theta}^*$:

$$0 = \nabla_{\boldsymbol{\theta}} P_N f(\hat{\boldsymbol{\theta}}_{N,M}; \mathbf{x}, \mathbf{v}_1^M)$$

$$= P_N \nabla_{\boldsymbol{\theta}} f(\boldsymbol{\theta}^*; \mathbf{x}, \mathbf{v}_1^M) + P_N\left(\nabla_{\boldsymbol{\theta}}^2 f(\boldsymbol{\theta}^*; \mathbf{x}, \mathbf{v}_1^M) + E_{\hat{\boldsymbol{\theta}}_{N,M}, \mathbf{x}, \mathbf{v}_1^M}\right)(\hat{\boldsymbol{\theta}}_{N,M} - \boldsymbol{\theta}^*), \quad (24)$$

where $\|E_{\hat{\boldsymbol{\theta}}_{N,M},\mathbf{x},\mathbf{v}_1^M}\|_F \leq L(\mathbf{x}, \mathbf{v}_1^M) \|\hat{\boldsymbol{\theta}}_{N,M} - \boldsymbol{\theta}^*\|_2$ from Lemma 4 and Taylor expansion of vector-valued functions. Combining with the law of large numbers, we have

$$P_N \nabla_{\boldsymbol{\theta}}^2 f(\boldsymbol{\theta}^*; \mathbf{x}, \mathbf{v}_1^M) = \mathbb{E}_{p_d, p_{\mathbf{v}}}[\nabla_{\boldsymbol{\theta}}^2 f(\boldsymbol{\theta}^*; \mathbf{x}, \mathbf{v}_1^M)] + o_p(1)$$

and

$$\left\| P_N E_{\hat{\boldsymbol{\theta}}_{N,M}} \right\|_F \leq \mathbb{E}_{p_d, p_{\mathbf{v}}}[L(\mathbf{x}, \mathbf{v}_1^M)] \left\| \hat{\boldsymbol{\theta}}_{N,M} - \boldsymbol{\theta}^* \right\|_2 + o_p(1) = o_p(1) + o_p(1) = o_p(1),$$

where we used $\mathbb{E}[L(\mathbf{x}, \mathbf{v}_1^M)] \leq \sqrt{\mathbb{E}[L^2(\mathbf{x}, \mathbf{v}_1^M)]} < \infty$ (Lemma 4) and the consistency of $\hat{\boldsymbol{\theta}}_{N,M}$ (Theorem 2). Now returning to (24), we get

$$0 = P_N \nabla_{\boldsymbol{\theta}} f(\boldsymbol{\theta}^*; \mathbf{x}, \mathbf{v}_1^M) + \left(\mathbb{E}_{p_d, p_{\mathbf{v}}}[\nabla_{\boldsymbol{\theta}}^2 f(\boldsymbol{\theta}^*; \mathbf{x}, \mathbf{v}_1^M)] + o_p(1) \right) (\hat{\boldsymbol{\theta}}_{N,M} - \boldsymbol{\theta}^*)$$

$$\Leftrightarrow \left(\nabla_{\boldsymbol{\theta}}^2 J(\boldsymbol{\theta}^*; p_{\mathbf{v}}) + o_p(1) \right) \sqrt{N} (\hat{\boldsymbol{\theta}}_{N,M} - \boldsymbol{\theta}^*) = -\sqrt{N} P_N \nabla_{\boldsymbol{\theta}} f(\boldsymbol{\theta}^*; \mathbf{x}, \mathbf{v}_1^M).$$

But of course, the central limit theorem and Lemma 5 yield

$$-\sqrt{N} P_N \nabla_{\boldsymbol{\theta}} f(\boldsymbol{\theta}^*; \mathbf{x}, \mathbf{v}_1^M) \xrightarrow{d} \mathcal{N}(0, \mathrm{Var}_{p_d, p_{\mathbf{v}}}\left[\nabla_{\boldsymbol{\theta}} f(\boldsymbol{\theta}^*; \mathbf{x}, \mathbf{v}_1^M) \right])$$

$$= \mathcal{N}\left(0, \sum_{i,j,p,q} \left[\left(1 - \frac{1}{M} \right) \Sigma_{ij} \Sigma_{pq} + \frac{1}{M} \mathfrak{S}_{ijpq} \right] \mathfrak{V}_{ijpq} \right).$$

Then, Slutsky's theorem gives the desired result

$$\sqrt{N} (\hat{\boldsymbol{\theta}}_{N,M} - \boldsymbol{\theta}^*) \xrightarrow{d}$$

$$\mathcal{N}\left(0, \left(\nabla_{\boldsymbol{\theta}}^2 J(\boldsymbol{\theta}^*; p_{\mathbf{v}}) \right)^{-1} \left(\sum_{i,j,p,q} \left[\left(1 - \frac{1}{M} \right) \Sigma_{ij} \Sigma_{pq} + \frac{1}{M} \mathfrak{S}_{ijpq} \right] \mathfrak{V}_{ijpq} \right) \left(\nabla_{\boldsymbol{\theta}}^2 J(\boldsymbol{\theta}^*; p_{\mathbf{v}}) \right)^{-1} \right).$$

In particular, if $p_{\mathbf{v}} \sim \mathcal{N}(0, I)$ or $p_{\mathbf{v}} \sim \mathcal{U}(\{\pm 1\}^D)$, we have $J(\boldsymbol{\theta}^*; p_{\mathbf{v}}) = J(\boldsymbol{\theta}^*)$, and therefore $\nabla_{\boldsymbol{\theta}}^2 J(\boldsymbol{\theta}^*; p_{\mathbf{v}}) = \nabla_{\boldsymbol{\theta}}^2 J(\boldsymbol{\theta}^*)$. We can apply Lemma 5 to conclude the simplified expressions for the asymptotic variance.

$\square$

Corollary 1 (Consistency and asymptotic normality of score matching). *Under similar assumptions used in Theorem 2 and Theorem 3, we can also conclude that the score matching estimator $\hat{\boldsymbol{\theta}}_N \triangleq \arg\min_{\boldsymbol{\theta} \in \Theta} \hat{J}(\boldsymbol{\theta}; \mathbf{x})$ is consistent*

$$\hat{\boldsymbol{\theta}}_N \xrightarrow{p} \boldsymbol{\theta}^*$$

and asymptotically normal

$$\sqrt{N} (\hat{\boldsymbol{\theta}}_N - \boldsymbol{\theta}^*) \xrightarrow{d} \mathcal{N}\left(0, \left(\nabla_{\boldsymbol{\theta}}^2 J(\boldsymbol{\theta}^*) \right)^{-1} \left(\sum_{ij} V_{ij} \right) \left(\nabla_{\boldsymbol{\theta}}^2 J(\boldsymbol{\theta}^*) \right)^{-1} \right).$$

Proof. Note that

$$\mathrm{Var}_{p_d}[\nabla_{\boldsymbol{\theta}} f(\boldsymbol{\theta}^*; \mathbf{x})] = \mathbb{E}_{p_d}[\nabla_{\boldsymbol{\theta}} f(\boldsymbol{\theta}^*; \mathbf{x}) \nabla_{\boldsymbol{\theta}} f(\boldsymbol{\theta}^*; \mathbf{x})^\mathsf{T}]$$

$$= \mathbb{E}_{p_d}\left[\left(\sum_i \nabla_{\boldsymbol{\theta}} \partial_i \partial_i l_m + \frac{1}{2} \nabla_{\boldsymbol{\theta}}(\partial_i l_m \partial_i l_m) \right) \left(\sum_j \nabla_{\boldsymbol{\theta}} \partial_j \partial_j l_m + \frac{1}{2} \nabla_{\boldsymbol{\theta}}(\partial_j l_m \partial_j l_m) \right)^\mathsf{T} \right]$$

$$= \sum_{ij} \mathbb{E}_{p_d}\left[\left(\nabla_{\boldsymbol{\theta}} \partial_i \partial_i l_m + \frac{1}{2} \nabla_{\boldsymbol{\theta}}(\partial_i l_m \partial_i l_m) \right) \left(\nabla_{\boldsymbol{\theta}} \partial_j \partial_j l_m + \frac{1}{2} \nabla_{\boldsymbol{\theta}}(\partial_j l_m \partial_j l_m) \right)^\mathsf{T} \right]$$

$$= \sum_{ij} V_{ij}$$

The other part of the proof is similar to that of Theorem 2 and Theorem 3 and is thus obmitted. $\square$

B.5 NOISE CONTRASTIVE ESTIMATION

Proposition 1. *Define*

$$J_{NCE}(\boldsymbol{\theta}) \triangleq -\mathbb{E}_{p_d}[\log h(\mathbf{x}; \boldsymbol{\theta})] - \mathbb{E}_{p_n}[\log(1 - h(\mathbf{x}; \boldsymbol{\theta}))]$$

where

$$h(\mathbf{x}; \boldsymbol{\theta}) \triangleq \frac{p_m(\mathbf{x}; \boldsymbol{\theta})}{p_m(\mathbf{x}; \boldsymbol{\theta}) + p_m(\mathbf{x} - \mathbf{v}; \boldsymbol{\theta})}$$

$$p_n(\mathbf{x}) = p_d(\mathbf{x} + \mathbf{v}).$$

Then when $\|v\|_2 \to 0$*, we have*

$$J_{NCE}(\boldsymbol{\theta}) = 2\log 2 + \frac{1}{4}\mathbb{E}_{p_d}\left[\mathbf{v}^\mathsf{T}\nabla^2 \log p_m(\mathbf{x}; \boldsymbol{\theta})\mathbf{v} + \frac{1}{2}(\nabla \log p_m(\mathbf{x}; \boldsymbol{\theta})^\mathsf{T}\mathbf{v})^2\right] + o(\|\mathbf{v}\|_2^2)$$

Proof. Using Taylor expansion, we can immediately get

$$\log p_m(\mathbf{x} + \mathbf{v}; \boldsymbol{\theta}) = \log p_m(\mathbf{x}; \boldsymbol{\theta}) + \nabla \log p_m(\mathbf{x}; \boldsymbol{\theta})^\mathsf{T}\mathbf{v} + \frac{1}{2}\mathbf{v}^\mathsf{T}\nabla^2 \log p_m(\mathbf{x}; \boldsymbol{\theta})\mathbf{v} + o(\|\mathbf{v}\|_2^2).$$

Next, observe that

$$\log(p_m(\mathbf{x}; \boldsymbol{\theta}) + p_m(\mathbf{x} + \mathbf{v}; \boldsymbol{\theta})) = \log p_m(\mathbf{x}; \boldsymbol{\theta}) + \log\left(1 + \exp\{\log p_m(\mathbf{x} + \mathbf{v}; \boldsymbol{\theta}) - \log p_m(\mathbf{x}; \boldsymbol{\theta})\}\right)$$

$$= \log p_m(\mathbf{x}; \boldsymbol{\theta}) + \log\left(1 + \exp\left\{\nabla \log p_m(\mathbf{x}; \boldsymbol{\theta})^\mathsf{T}\mathbf{v} + \frac{1}{2}\mathbf{v}^\mathsf{T}\nabla^2 \log p_m(\mathbf{x}; \boldsymbol{\theta})\mathbf{v} + o(\|\mathbf{v}\|_2^2)\right\}\right)$$

$$= \log p_m(\mathbf{x}; \boldsymbol{\theta}) + \log 2 + \frac{1}{2}\left[\nabla \log p_m(\mathbf{x}; \boldsymbol{\theta})^\mathsf{T}\mathbf{v} + \frac{1}{2}\mathbf{v}^\mathsf{T}\nabla^2 \log p_m(\mathbf{x}; \boldsymbol{\theta})\mathbf{v}\right] + \frac{1}{8}(\nabla \log p_m(\mathbf{x}; \boldsymbol{\theta})^\mathsf{T}\mathbf{v})^2 + o(\|\mathbf{v}\|_2^2).$$

Similarly, we have

$$\log(p_m(\mathbf{x}; \boldsymbol{\theta}) + p_m(\mathbf{x} - \mathbf{v}; \boldsymbol{\theta}))$$

$$= \log p_m(\mathbf{x}; \boldsymbol{\theta}) + \log 2 + \frac{1}{2}\left[-\nabla \log p_m(\mathbf{x}; \boldsymbol{\theta})^\mathsf{T}\mathbf{v} + \frac{1}{2}\mathbf{v}^\mathsf{T}\nabla^2 \log p_m(\mathbf{x}; \boldsymbol{\theta})\mathbf{v}\right] + \frac{1}{8}(\nabla \log p_m(\mathbf{x}; \boldsymbol{\theta})^\mathsf{T}\mathbf{v})^2 + o(\|\mathbf{v}\|_2^2).$$

Finally, note that

$$J_{\text{NCE}}(\boldsymbol{\theta}) = -\mathbb{E}_{p_d}[\log h(\mathbf{x}; \boldsymbol{\theta}) + \log(1 - h(\mathbf{x} + \mathbf{v}; \boldsymbol{\theta}))]$$

$$= -\mathbb{E}_{p_d}[\log p_m(\mathbf{x}; \boldsymbol{\theta}) - \log(p_m(\mathbf{x}; \boldsymbol{\theta}) + p_m(\mathbf{x} - \mathbf{v}; \boldsymbol{\theta}))] - \mathbb{E}_{p_d}[\log p_m(\mathbf{x}; \boldsymbol{\theta}) - \log(p_m(\mathbf{x}; \boldsymbol{\theta}) + p_m(\mathbf{x} + \mathbf{v}; \boldsymbol{\theta}))]$$

$$= 2\log 2 + \frac{1}{4}\mathbb{E}_{p_d}\left[\mathbf{v}^\mathsf{T}\nabla^2 \log p_m(\mathbf{x}; \boldsymbol{\theta})\mathbf{v} + \frac{1}{2}(\nabla \log p_m(\mathbf{x}; \boldsymbol{\theta})^\mathsf{T}\mathbf{v})^2\right] + o(\|\mathbf{v}\|_2^2),$$

as desired. $\square$

C ADDITIONAL DETAILS OF EXPERIMENTS

C.1 KERNEL EXPONENTIAL FAMILIES

Model The kernel exponential family is a class of densities with unnormalized log density given by $\log \tilde{p}_f(\mathbf{x}) = f(\mathbf{x}) + \log q_0(\mathbf{x})$. Here, q_0 is a fixed function and f belongs to a reproducing kernel Hilbert space $\mathcal{H}$, with kernel k (Canu & Smola, 2006; Sriperumbudur et al., 2017). We see this is a member of the exponential family by using reproducing property, $f(\mathbf{x}) = \langle f, k(x, \cdot)\rangle_{\mathcal{H}}$. Rewriting the density, the model has natural parameter f and sufficient statistic $k(\mathbf{x}, \cdot)$:

$$\tilde{p}_f(\mathbf{x}) = \exp(f(\mathbf{x}))q_0(\mathbf{x}) = \exp(\langle f, k(x, \cdot)\rangle_{\mathcal{H}}))q_0(\mathbf{x})$$

To improve computational cost of learning f, Sutherland et al. (2018) use a Nyström-type lite approximation, selecting L inducing points $\mathbf{z}_l$, and f of the form:

$$f(\mathbf{x}) = \sum_{l=1}^{L} \alpha_l k(\mathbf{x}, \mathbf{z}_l)$$

We compare training using our objective against deep kernel exponential family (DKEF) models trained using exact score matching in Wenliang et al. (2018).

The kernel $k(\mathbf{x}, \mathbf{y})$ is a mixture of $R = 3$ Gaussian kernels, with features extracted by a neural network, $\phi_{w_r}(\cdot)$, length scales σ_r, and nonnegative mixture coefficients ρ_r. The neural network is a three layer fully connected network with a skip connection from the input to output layers and softplus nonlinearities. Each hidden layer has 30 neurons. We have:

$$k_w(\mathbf{x}, \mathbf{y}) = \sum_{r=1}^{R} \rho_r \exp\left(-\frac{1}{2\sigma_r^2} \|\phi_{w_r}(\mathbf{x}) - \phi_{w_r}(\mathbf{y})\|^2 \right).$$

When training DKEF models, Wenliang et al. (2018) note that it is possible to analytically minimize the score matching loss over α because the objective is quadratic in α. As a result, models are trained in a two step procedure: α is analytically minimized over a training minibatch, then the loss is computed over a validation minibatch. When training models, the analytically minimized α is treated as function of the other parameters. By doing this, Wenliang et al. (2018) can also directly optimize the coefficient $\lambda_{\boldsymbol{\alpha}}$ of a L2 regularization loss on $\boldsymbol{\alpha}$. This regularization coefficient is initalized to 0.01, and is trained. (More details about the two-step optimization procedure can be found in Wenliang et al. (2018), which also includes a finalization stage for $\boldsymbol{\alpha}$).

A similar closed form for sliced score matching, denoising score matching, approximate backpropagation, and curvature propagation can be derived. The derivation for sliced score matching is presented below for completeness.

Proposition 2. *Consider the loss*

$$\hat{J}(\boldsymbol{\theta}, \lambda_{\boldsymbol{\alpha}}; \mathbf{x}_1^N, \mathbf{v}_{11}^{NM}) = \hat{J}(\boldsymbol{\theta}; \mathbf{x}_1^N, \mathbf{v}_{11}^{NM}) + \frac{1}{2} \lambda_{\boldsymbol{\alpha}} \|\boldsymbol{\alpha}\|_2^2$$

where

$$\hat{J}(\boldsymbol{\theta}; \mathbf{x}_1^N, \mathbf{v}_{11}^{NM}) = \frac{1}{N} \frac{1}{M} \sum_{i=1}^{N} \sum_{j=1}^{M} \left[\mathbf{v}_{ij}^{\mathsf{T}} \nabla^2 \log p_m(\mathbf{x}_i) \mathbf{v}_{ij} + \frac{1}{2} \left(\mathbf{v}_{ij}^{\mathsf{T}} \nabla \log p_m(\mathbf{x}_i) \right)^2 \right].$$

For fixed k, $\mathbf{z}$, and $\lambda_{\boldsymbol{\alpha}}$, as long as $\lambda_{\boldsymbol{\alpha}} > 0$ then the optimal $\boldsymbol{\alpha}$ is

$$\boldsymbol{\alpha}(\lambda_{\boldsymbol{\alpha}}, k, \mathbf{z}, \mathbf{x}_1^N, \mathbf{v}_{11}^{NM}) = \arg\min_{\boldsymbol{\alpha}} \hat{J}(\boldsymbol{\theta}, \lambda_{\boldsymbol{\alpha}}; \mathbf{x}_1^N, \mathbf{v}_{11}^{NM}) = -\left(\boldsymbol{G} + \lambda_{\alpha} \boldsymbol{I} \right)^{-1} \boldsymbol{b}$$

$$G_{l,l'} = \frac{1}{N} \frac{1}{M} \sum_{i=1}^{N} \sum_{j=1}^{M} \left(\mathbf{v}_{ij}^{\mathsf{T}} \nabla k(\mathbf{x}_i, \mathbf{z}_l) \right) \left(\mathbf{v}_{ij}^{\mathsf{T}} \nabla k(\mathbf{x}_i, \mathbf{z}_{l'}) \right)$$

$$b_l = \frac{1}{N} \frac{1}{M} \sum_{i=1}^{N} \sum_{j=1}^{M} \mathbf{v}_{ij}^{\mathsf{T}} \nabla^2 k(\mathbf{x}_i, \mathbf{z}_l) \mathbf{v}_{ij} + \left(\mathbf{v}_{ij}^{\mathsf{T}} \nabla \log q_0(\mathbf{x}_i) \right) \left(\mathbf{v}_{ij}^{\mathsf{T}} \nabla k(\mathbf{x}_i, \mathbf{z}_l) \right).$$

Proof. The derivation follows very similarly to Proposition 3 in Wenliang et al. (2018). We will show that the loss is quadratic in $\boldsymbol{\alpha}$. Note that

$$\frac{1}{N} \frac{1}{M} \sum_{i=1}^{N} \sum_{j=1}^{M} \mathbf{v}_{ij}^{\mathsf{T}} \nabla^2 \log p_m(\mathbf{x}_i) \mathbf{v}_{ij} = \frac{1}{N} \frac{1}{M} \sum_{i=1}^{N} \sum_{j=1}^{M} \left[\sum_{m=1}^{M} \alpha_l \mathbf{v}_{ij}^{\mathsf{T}} \nabla^2 k(\mathbf{x}_i, \mathbf{z}_l) \mathbf{v}_{ij} \right] + \text{const}$$

$$= \boldsymbol{\alpha}^{\mathsf{T}} \left[\frac{1}{N} \frac{1}{M} \sum_{i=1}^{N} \sum_{j=1}^{M} \mathbf{v}_{ij}^{\mathsf{T}} \nabla^2 k(\mathbf{x}_i, \mathbf{z}_l) \mathbf{v}_{ij} \right]_l + \text{const}$$

$$\frac{1}{N}\frac{1}{M}\sum_{i=1}^{N}\sum_{j=1}^{M}\frac{1}{2}\left(\mathbf{v}_{ij}^{\mathsf{T}}\nabla\log p_m(\mathbf{x}_i)\right)^2 = \frac{1}{N}\frac{1}{M}\sum_{i=1}^{N}\sum_{j=1}^{M}\frac{1}{2}\left(\sum_{m,m'=1}^{M}\alpha_l\alpha_{m'}\left(\mathbf{v}_{ij}^{\mathsf{T}}\nabla k(\mathbf{x}_i,\mathbf{z}_l)\right)\left(\mathbf{v}_{ij}^{\mathsf{T}}\nabla k(\mathbf{x}_i,\mathbf{z}_{l'})\right)\right.$$

$$\left.+2\sum_{m=1}^{M}\alpha_l\left(\mathbf{v}_{ij}^{\mathsf{T}}\nabla\log q_0(\mathbf{x}_i)\right)\left(\mathbf{v}_{ij}^{\mathsf{T}}\nabla k(\mathbf{x}_i,\mathbf{z}_l)\right)+\left(\mathbf{v}_{ij}^{\mathsf{T}}\nabla\log q_0(\mathbf{x}_i)\right)^2\right)$$

$$=\frac{1}{2}\boldsymbol{\alpha}^{\mathsf{T}}\boldsymbol{G}\boldsymbol{\alpha}+\boldsymbol{\alpha}^{\mathsf{T}}\left[\frac{1}{N}\frac{1}{M}\sum_{i=1}^{N}\sum_{j=1}^{M}\left(\mathbf{v}_{ij}^{\mathsf{T}}\nabla\log q_0(\mathbf{x}_i)\right)\left(\mathbf{v}_{ij}^{\mathsf{T}}\nabla k(\mathbf{x}_i,\mathbf{z}_l)\right)\right]+\text{const.}$$

Thus the overall optimization problem is

$$\boldsymbol{\alpha}(\lambda_{\boldsymbol{\alpha}},k,\mathbf{z},\mathbf{x}_1^N,\mathbf{v}_{11}^{NM})=\arg\min_{\boldsymbol{\alpha}}\hat{J}(\boldsymbol{\theta},\lambda_{\boldsymbol{\alpha}};\mathbf{x}_1^N,\mathbf{v}_{11}^{NM})$$

$$=\arg\min_{\boldsymbol{\alpha}}\frac{1}{2}\boldsymbol{\alpha}^{\mathsf{T}}\left(\boldsymbol{G}+\lambda_{\boldsymbol{\alpha}}\boldsymbol{I}\right)\boldsymbol{\alpha}+\boldsymbol{\alpha}^{\mathsf{T}}\boldsymbol{b}.$$

Because $\lambda_\alpha > 0$ and $\boldsymbol{G}$ is positive semidefinite, the matrix in parentheses is strictly positive definite, and the claimed result follows directly from standard vector calculus. $\qquad\square$

Hyperparameters RedWine and WhiteWine are dequantized by adding uniform noise to each dimension in the range $[-d,d]$ where d is the median distance between two values for that dimension. For each dataset, 10% of the entire data was used as testing, and 10% of the remaining was used for validation. PCA whitening is applied to the data. Noise of standard deviation 0.05 is added as part of preprocessing.

The DKEF models have $R=3$ Gaussian kernels. Each feature extractor is a 3-layer neural network with a skip connnection from the input to putput, with 30 hidden neurons per layer. Weights were initialized from a Gaussian distribution with standard deviation equal to $\frac{1}{\sqrt{30}}$. Length scales σ_r were initialized to 1.0, 3.3 and 10.0. We use $L=200$ trainable inducing points, which were initialized from training data.

Models are trained using an Adam optimizer, with learning rate 10^{-2}. A batch size of 200 is used, with 100 points for computing $\boldsymbol{\alpha}$, and 100 for computing the loss. Models are stopped after validation loss does not improve for 200 steps.

For denoising score matching, we perform a grid search with values [0.02, 0.04, 0.06, 0.08, 0.10, 0.12, 0.14, 0.16, 0.20, 0.24, 0.28, 0.32, 0.40, 0.48, 0.56, 0.64, 1.28]. We train models for each value of σ using two random seeds, and pick the σ with the best average validation score matching loss. For curvature propagation, one noise sample is used to match the performance of sliced score matching.

Log-likelihoods Log-likelihoods are presented below. They are estimated using AIS, using a proposal distribution $\mathcal{N}(0,2I)$, using 1,000,000 samples.
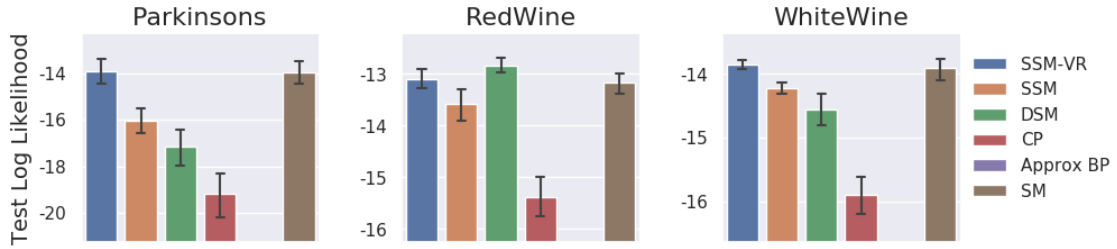

Figure 3: Log likelihoods after training DKEF models on UCI datasets with different loss functions; higher is better. Results for approximate backprapagation are not shown because LLs were smaller than -10^6.

Name	Configuration	Algorithm
Encoder	Linear(784, 256), Tanh Linear(256, 256), Tanh Linear(256, $D_{\mathbf{z}}$)	ELBO VAE, WAE
Implicit Encoder	Linear(784 + $D_{\boldsymbol{\epsilon}}$, 256), Tanh Linear(256, 256), Tanh Linear(256, $D_{\mathbf{z}}$)	Implicit VAE
Decoder	Linear($D_{\mathbf{z}}$, 256), Tanh Linear(256, 256), Tanh Linear(256, 784), Sigmoid	All
Score Estimator	Linear(784 + $D_{\mathbf{z}}$, 256), Tanh Linear(256, 256), Tanh Linear(256, $D_{\mathbf{z}}$)	Implicit VAE
Score Estimator	Linear($D_{\mathbf{z}}$, 256), Tanh Linear(256, 256), Tanh Linear(256, $D_{\mathbf{z}}$)	WAE

Table 8: Architectures on MNIST. In our models, $D_{\boldsymbol{\epsilon}} = D_{\mathbf{z}}$. $D_{\mathbf{z}}$ takes the values 8 and 32 in different experiments.

C.2   NICE

Hyperparameters and Model Architecture   The model has four coupling layers, each with five hidden layers, for a total of 20 hidden layers, as well as a final scale layer (Dinh et al., 2015). Softplus nonlinearities are used between hidden layers.

Models are trained using the Adam optimizer with learning rate 10^{-3} for 100 epochs. The best checkpoint on exact score matching loss, evaluation every 100 iterations, is used to report test set performance. We use a batch size of 128.

Data are dequantized by adding uniform noise in the range $[-\frac{1}{512}, \frac{1}{512}]$, clipped to be in the range $[-0.001, 0.001]$, and then transformed using a logit transformation $\log(x) - \log(1 - x)$. 90% of the training set is used for training, and 10% for validation, and the standard test set is used.

For grid search for the optimal value of σ, eight values are used: [0.01, 0.05, 0.10, 0.20, 0.28, 0.50, 1.00, 1.50]. We also evaluate $\sigma = 1.74$, chosen by the heuristic in Saremi et al. (2018). The model with the best performance on validation score matching loss is used. Only nine values of σ are evaluated because training each model takes approximately two hours.

C.3   SCORE ESTIMATION FOR IMPLICIT DISTRIBUTIONS

Architectures   We put the architectures of all networks used in the MNIST and CelebA experiments in Tab. 8 and Tab. 9 respectively.

Training   For MNIST experiments, we use RMSProp optimizer with a learning rate of 0.001 for all methods. On CelebA, the learning rate is changed to 0.0001. All algorithms are trained for 100000 iterations with a batch size of 128.

Samples   All samples are generated after 100000 training iterations.

D   VARIANCE REDUCTION

Below we discuss approaches to reduce the variance of $\hat{J}(\boldsymbol{\theta}; \mathbf{x}_1^N, \mathbf{v}_{11}^{NM})$, which can lead to better performance in practice. The most naïve approach, of course, is using a larger M to compute $\hat{J}(\boldsymbol{\theta}; \mathbf{x}_1^N, \mathbf{v}_{11}^{NM})$. However, this requires more computation and when M is close to the data dimension, sliced score matching will lose its computational advantage over score matching.

An alternative approach is to leverage control variates (Owen, 2013). A control variate is a random variable whose expectation is tractable, and is highly correlated with another random variable without a tractable expectation. Define

Name	Configuration	Algorithm
Encoder	5×5 conv; m maps; stride 2×2; padding 2, ReLU 5×5 conv; $2m$ maps; stride 2×2; padding 2, ReLU 5×5 conv; $4m$ maps; stride 2×2; padding 2, ReLU 5×5 conv; $8m$ maps; stride 2×2; padding 2, ReLU 512 Dense, ReLU $D_{\mathbf{z}}$ Dense	ELBO VAE, WAE
Implicit Encoder	concat $[\mathbf{x}, \text{ReLU}(\text{Dense}(\boldsymbol{\epsilon}))]$ along channels 5×5 conv; m maps; stride 2×2; padding 2, ReLU 5×5 conv; $2m$ maps; stride 2×2; padding 2, ReLU 5×5 conv; $4m$ maps; stride 2×2; padding 2, ReLU 5×5 conv; $8m$ maps; stride 2×2; padding 2, ReLU 512 Dense, ReLU $D_{\mathbf{z}}$ Dense	Implicit VAE
Decoder	Dense, ReLU 5×5 conv$^{\intercal}$; $4m$ maps; stride 2×2; padding 2; out padding 1, ReLU 5×5 conv$^{\intercal}$; $2m$ maps; stride 2×2; padding 2; out padding 1, ReLU 5×5 conv$^{\intercal}$; $1m$ maps; stride 2×2; padding 2; out padding 1, ReLU 5×5 conv$^{\intercal}$; c maps; stride 2×2; padding 2; out padding 1, Tanh	All
Score Estimator	concat $[\mathbf{x}, \text{ReLU}(\text{Dense}(\mathbf{z}))]$ along channels 5×5 conv; m maps; stride 2×2; padding 2, ReLU 5×5 conv; $2m$ maps; stride 2×2; padding 2, ReLU 5×5 conv; $4m$ maps; stride 2×2; padding 2, ReLU 5×5 conv; $8m$ maps; stride 2×2; padding 2, ReLU 512 Dense, ReLU $D_{\mathbf{z}}$ Dense	Implicit VAE
Score Estimator	Reshape(ReLU(Dense($\mathbf{z}$))]) to 1 channel 5×5 conv; m maps; stride 2×2; padding 2, ReLU 5×5 conv; $2m$ maps; stride 2×2; padding 2, ReLU 5×5 conv; $4m$ maps; stride 2×2; padding 2, ReLU 5×5 conv; $8m$ maps; stride 2×2; padding 2, ReLU 512 Dense, ReLU $D_{\mathbf{z}}$ Dense	WAE

Table 9: Architectures on CelebA. In our models, $D_{\boldsymbol{\epsilon}} = D_{\mathbf{z}}$. $D_{\mathbf{z}}$ takes the values 8 or 32 in different experiments.

$c(\boldsymbol{\theta}; \mathbf{x}, \mathbf{v}) \triangleq \frac{1}{2}(\mathbf{v}^{\intercal}\mathbf{s}_m(\mathbf{x}; \boldsymbol{\theta}))^2$. Note that when $p_{\mathbf{v}}$ is a multivariate standard normal or multivariate Rademacher distribution, $c(\boldsymbol{\theta}; \mathbf{x}, \mathbf{v})$ will have a tractable expectation, *i.e.*,

$$\mathbb{E}_{p_{\mathbf{v}}}[c(\boldsymbol{\theta}; \mathbf{x}, \mathbf{v})] = \frac{1}{2} \left\| \mathbf{s}_m(\mathbf{x}; \boldsymbol{\theta}) \right\|_2^2,$$

which is easily computable. Now let $\beta(\mathbf{x})c(\boldsymbol{\theta}; \mathbf{x}, \mathbf{v})$ be our control variate, where $\beta(\mathbf{x})$ is a function to be determined. Due to the structural similarity between $\beta(\mathbf{x})c(\boldsymbol{\theta}; \mathbf{x}, \mathbf{v})$ and $\hat{J}(\boldsymbol{\theta}; \mathbf{x}_1^N, \mathbf{v}_{11}^{NM})$, it is easy to believe that $\beta(\mathbf{x})c(\boldsymbol{\theta}; \mathbf{x}, \mathbf{v})$ can be a correlated control variate with an appropriate $\beta(\mathbf{x})$. We thus consider the following objective

$$\hat{J}_{\text{vr}}(\boldsymbol{\theta}; \mathbf{x}_1^N, \mathbf{v}_{11}^{NM}) \triangleq \hat{J}(\boldsymbol{\theta}; \mathbf{x}_1^N, \mathbf{v}_{11}^{NM}) - \frac{1}{N}\sum_{i=1}^{N}\beta(\mathbf{x}_i)\left(\frac{1}{M}\sum_{j=1}^{M}c(\boldsymbol{\theta}; \mathbf{x}_i, \mathbf{v}_{ij}) - \frac{1}{2}\left\|\mathbf{s}_m(\mathbf{x}_i; \boldsymbol{\theta})\right\|_2^2\right).$$

Note that $\mathbb{E}[\hat{J}_{\text{vr}}(\boldsymbol{\theta}; \mathbf{x}_1^N, \mathbf{v}_{11}^{NM})] = J(\boldsymbol{\theta}; p_{\mathbf{v}})$. The theory of control variates guarantees the existence of $\beta(\mathbf{x})$ that can reduce the variance. In practice, there can be many heuristics of choosing $\beta(\mathbf{x})$, and we found that $\beta(\mathbf{x}) \equiv 1$ can often be a good choice in our experiments.

E   PSEUDOCODE

Algorithm 2 Score Matching

Input: $\tilde{p}_m(\cdot; \boldsymbol{\theta}), \mathbf{x}$
1: $\mathbf{s}_m \leftarrow \mathrm{grad}(\log \tilde{p}_m(\mathbf{x}; \boldsymbol{\theta}), \mathbf{x})$
2: $J \leftarrow \frac{1}{2} \|\mathbf{s}_m\|_2^2$
3: **for** $d \leftarrow 1$ to D **do**   ▷ For each diagonal entry
4:     $(\nabla_{\mathbf{x}} \mathbf{s}_m)_d \leftarrow \mathrm{grad}((\mathbf{s}_m)_d, \mathbf{x})_d$
5:     $J \leftarrow J + (\nabla_{\mathbf{x}} \mathbf{s}_m)_d$
6: **end for**
7: **return** J